INVESTIGATE THE USE OF STRAIN GAUGE TECHNOLOGY FOR THE DETERMINATION OF THE MECHANICAL CHARACTERISTICS OF POLYPROPYLENE ANKLE-FOOT ORTHOSES

by

ENRICA PAPI

September 2008

Thesis submitted in partial fulfilment of the requirements for the degree of Master of Science in Bioengineering, University of Strathclyde

Bioengineering Unit

University of Strathclyde

Glasgow

COPYRIGHT

ABSTRACT

Ankle-Foot Orthoses (AFOs) are devices applied to the foot and lower leg when ankle joint stability has been lost, commonly through, upper and lower motor neuron lesions resulting in gait abnormalities. Conventional leather and metal AFOs have been largely superseded by plastic devices in recent years, especially made from polypropylene (PP). To date the design of AFOs is mainly based on empirical studies. A survey of the literature indicates that there is a dearth of experimental investigations in this area. Consequently, more research should be conducted on the mechanical characteristics of AFOs and their interaction with the limb in order to improve design criteria, performances and prescription of the orthoses.

The objective of this project was to assess the performance of strain gauges attached to polypropylene (PP) with the perspective of using them to determine orthotic loads and stresses generated in polypropylene AFOs during patient's activity.

Initially PP samples with an extensometer attached on them were tested following as far as possible the British Standard BS 527-1, with two different tensile test protocols on an Instron machine with the aim of investigating the material's viscoelastic nature.

Strain gauged samples were tested in tension at low (0.158 mm/min) and high strain rates (2.43 mm/min), in a stress range between 0-2 MPa. Investigation of two different bonding methods used for gauge foils installation on polypropylene was, thus, carried out to verify the most preferable technique. This was achieved by comparing strains measured by the strain gauges and the extensometer, attached to the side of the sample.

Results obtained by strain gauge testing showed that a better accuracy was achieved in polypropylene UV light pre-treated samples where strain gauges were attached with cyanoacrylate adhesive (10% difference at slow rate) rather than in samples in which M-Bond AE-10 adhesive was used (19% difference). The accuracy was found to be reduced at fast strain rate. Higher values of strains were measured by strain gauges than by the extensometer. Reasons for this unexpected result require more detailed investigations on viscoelastic properties of the adhesive and its interaction both with the sample and strain gauge backing foil, gauge lengths, and sample shape. A custom-made polypropylene AFO was strain gauged using UV light treatment and cyanoacrylate adhesive. Moments in the sagittal plane generated in the orthosis were calculated from strain gauge voltage outputs during one walking trial of a normal subject donned with the instrumented orthosis. The moment pattern obtained followed the expected plantar and dorsiflexion pattern for a normal subject during walking. More walking trials, however, should be conducted to provide repeatability in the results.

ACKNOWLEDGEMENTS

I would like to thank my supervisors, Bill Spence and Stephan Solomonidis, for their guidance in the completion of this thesis. My utmost gratitude goes in particular to my supervisor Stephan Solomonidis for his precious teachings, patience, helpfulness and enthusiasm that makes me forgetting all the hard work to complete this study. His continuous encouragements were greatly appreciated.

Thanks to all of those offer me their help in the Bioengineering Unit during this year. In particular I would like to thank Dave Smith and John Maclean for their time, help and patience with me, "my" funny strain gauges and polypropylene samples, but someone said "*If we knew what it was we were doing, it would not be called research, would it?*". Thanks!

Thanks to the Student Awards Agency for Scotland (SAAS) for the scholarship provided.

I don't have enough words to thank my adorable family for their endless support, boundless love and constant presence although the distance. To them I dedicate this thesis.

The sweetest thanks to my grandmother Gianna who keeps on calling me everyday defeating every scottish phone lines.

My gratitude to my other mums, Antonella and Emanuela, my indestructible grandfather Ciacci, my little cousin Laura for their invaluable encouragements and endless love. I would like to thank my grandmother Lara, as well, for her trust in me.

A smiling thanks to all the new friends met during this Glaswegians experience for let me enjoying the new life in an unknown city introducing me to the combination books and beers. A particular thanks to all of you who cheer me up in the last stressful period.

A big and loving thanks to my Urbino's friends, my own fan club, that *over the hill and far away* are able to make me not feel lonely in this new rainy city: thanks to my Liz for being my best friend, to the great Pagno, to the sweetie Mony, to the

inimitable Adry, to the little Sary, to the snowborders Pippo and Simo, to the engineer Maggio, the wise Andry and finally a grateful thanks to the precious Giachi.
A special thank to my "wife" Rammy for continuing partying with me through skipe, to my Cesena's family Camy and Sery for their priceless friendship.
A musical thanks to Bruno for constantly believing in me, to the discovered chef Manuel, to my favourite secretary Giacomo for his appreciated e-mails..... This list might continue but it is impossible to mention all the friends and people that everyday throughout this year join me in this experience and help me to make the best of it, a sparkling thanks to all of you.
Should I thank myself as well?!

"You may say I'm a dreamer, but I'm not the only one"

Glasgow 19/08/2008 Enrica

CONTENTS

CHAPTER 4

CHAPTER 5

CHAPTER 6

CHAPTER 1

INTRODUCTION

1.1 BACKGROUND AND OBJECTIVES OF THE STUDY

Orthoses are devices applied to modify the system of external forces and moments acting across a joint in a body segment, which is unable to control or resist these forces due to impairment or disease. The present study concentrates on ankle-foot orthoses (AFOs) which are devices applied to the foot and lower leg when ankle joint stability is compromised. They are commonly prescribed in the management of upper and lower motor neuron lesions resulting in gait abnormalities.

AFOs are amongst the most commonly prescribed categories of lower limb orthoses and, despite their small size and apparent simplicity, have proved disproportionately effective in enhancing the function of a wide range of patients group of all ages (Bowker et al, 1993).

Traditionally made from metal and leather, nowadays AFOs are made from thermoplastic materials resulting in more cosmetic and lighter devices. The most common plastics used for AFO manufacture is polypropylene (Showers et al., 1985).

For a correct management of lower limb deformities, an AFO should apply the required magnitude of forces without interfering with the patient ability to walk, provide a comfortable pressure distribution preventing soft tissues damaging (Bowker, 1987) and reduce energy expenditure while helping to approximate a normal gait pattern when a patient is fitted with the device (Lehmann, 1979). Therefore an understanding of the mechanical properties of AFOs is important to succeed in rehabilitation of impaired patients. The interaction between the orthosis and the patient's lower leg is also a relevant parameter when aiming for an enhanced AFO design.

The majority of experimental studies on AFO concentrates on the gait analysis of patients donned with the orthosis investigating the resulting gait pattern (Magora et al.,1968; Dieli et al.,1997; Chu, 1998,2000). These studies, however, are focused on particular scenarios, e.g. specific types of AFO and pathologies, without providing a large spectrum of data for improving the effectiveness of AFOs design. A better understanding of orthotic loads is required to make progress on orthosis prescription and design. Forces between the AFO and the lower leg during a gait cycle have been only studied theoretically so far (Leone, 1987; Bowker et al., 1993; Mc Hugh, 1999).

It is the first aim of this project to investigate the use of strain gauges attached on polypropylene samples with a view of using them to determine mechanical characteristics of plastic AFOs. Assessment of the biomechanical functions of AFOs can be achieved, in fact, by measuring gait forces and moment supported by the orthosis using an instrumented AFO and measuring the ground reaction forces with a forceplate. In turn this will also allow the estimation of anatomical forces on the patient's affected leg to be determined. With data acquired by the mentioned method, improvements in design criteria of an AFO should be accomplished.

However, a backward step is first required before moving forward to the loads analysis of the patient and plastic AFO system. The accuracy of strain gauges, intended to be used for measuring orthotics loads must be, in fact verified. Strain gauges technology was first used for this purpose by Chu (1996, 1998, 2000) but the accuracy of the methodology were not discussed. Melissa Webster (2006) then attempted to study strain gauges application to polypropylene. The latter investigation, however, does not provide conclusive results indicating whether strain gauges can be applied in order to study the biomechanical functions of AFOs.

The project described throughout the next chapters of this thesis investigates the doubts brought about by the mentioned study (Webster, 2006) to assess strain gauges accuracy on polypropylene. Strain gauging a plastic material in fact involves different critical aspects related to the material behaviour itself to be considered, comparing to when dealing with strain gauging a metal (Window, 1992). In addition the bonding technique to be used for attaching strain gauges to plastic materials is a

very important aspect in strain gauge accuracy and reliability. An investigation of the polypropylene viscoelastic nature therefore, was planned before evaluating the feasibility of using strain gauges for strains measurements on polypropylene.
Then it was planned to compare the performance of strain gauges with other strain measuring methods, such as exetensometry. Last aim of this project, as anticipated earlier, was to determine loads taken by the orthosis in a healthy subject fitted with a strain gauged polypropylene AFO.

1.2 ORGANISATION OF THE THESIS

The second chapter provides an introduction to the subject of orthotic devices, with particular regards to the lower limb orthoses biomechanics and functions. Clinical conditions which may be served by those orthotic devices are also described.
Chapter 3 concentrates on ankle-foot orthoses. Materials used for AFO manufacture are discussed together with the various designs so far developed. Secondly a brief introduction on gait analysis terminology, parameters and instrumentation used for this purpose is given to the reader. This will provide a better understanding of the subsequent part of this chapter which examines principal pathologies treated with AFOs. The chapter concludes with a review of the research conducted in this area to date.
Chapter 4 describes the methods and instrumentation used in the current study.
The fifth chapter illustrates experimental results obtained by the tests conducted on polypropylene samples and when performing the test on a subject fitted a strain gauged polypropylene AFO.
Discussions related to the results presented in chapter 5 are detailed in chapter 6.
Finally the conclusions and recommendations for future studies are provided in chapter 7.

CHAPTER 2

INTRODUCTION TO ORTHOSES

2.1 INTRODUCTION

The term orthoses, as defined by the International Standard Organization, refers to externally applied devices used to modify the structural and functional characteristics of the neuromuscular and skeletal system (ISO 8549-1, 1989).

These orthopaedic devices applied to a dysfunctioning body segment can be either static or dynamic. Thereby the use of terms such as splint, brace, or caliper is discouraged since they describe just static devices.

The terminology used in orthotics is based upon guidelines produced by collaboration among the American Academy of Orthopaedic Surgeons (AAOS), the Committee on Prosthetics Orthotics Education (CPOE), and the American Orthothics and Prosthetic Association (Lim, 1985).

This nomenclature is based on the joints the orthosis encompasses. The acronym AFO for ankle-foot orthosis, superseded the traditional short leg brace to describe the device that encompasses the foot and ankle joint extending to a point below the knee (Figure 2.1).

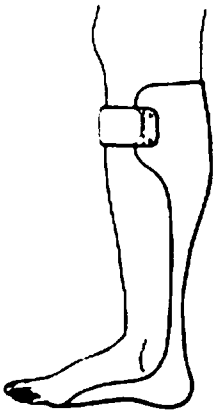

Figure 2.1: Ankle Foot Orthosis.

All orthoses operate by applying forces to the body in order to:

- *correct* deformities by re-aligning the limb;
- *control* motion of a limb segment;
- *compensate* for absent forces due to weakened or absent muscle power;
- *support* anatomical structures from weight bearing.

At least one 3 point-force system is applied by each device on a patient's limb to restore more normal functions in pathological situations.

The basic principles on the application of forces system between the body and the orthosis will be discussed in the next chapter with particular regards on AFOs.

This chapter aims at giving to the reader an introduction to clinical conditions which may be served by orthotic devices together with an overview of lower limb orthoses functions.

2.2 CLINICAL CONDITION TREATABLE WITH ORTHOTIC MANAGEMENT

Disorders or abnormalities of the neuromuscular skeletal system result in a reduction of patient's ambulatory ability and consequently requirement of orthotic devices.

A brief description of conditions that may necessitate the use of orthoses is given below.

2.2.1 Motor Neuron Disorders

One of the most common reasons of fitting an orthosis is the loss of stability through upper and lower motor neuron lesion.

Upper motor neuron lesions will result in muscle control dysfunction with the patient no longer able to dictate when muscles should contract. Muscles respond to a number of different stimuli resulting in involuntary patterns of motion. This abnormal increase in muscle tone is referred to spasticity. Muscles usually involved are antigravity muscles, such as hamstrings, quadriceps and adductors. Individual's gait becomes stiff and slow.

Several categories of patient exhibit these characteristics; however one of the most important groups is children with cerebral palsy. Cerebral palsy is a disorder that affects voluntary motor performance and arises in infancy or childhood as a result of prenatal trauma, drug exposure, or a congenital defect (Martini, 2006) There are three main types of cerebral palsy: spastic, athetoid and ataxic. The abnormalities in motor skill derived by these diseases can be treated by the use of an orthosis to control involuntary motion, foot positioning and correct deformities.

Lower motor neuron lesions, on the contrary, is usually associated with flaccid paralysis, caused by reduced muscle tone. Either voluntary or reflex muscle activity is decreased. Atrophy or wasting of the affected muscles can be seen. The reduction in muscle tone can be compensated by an orthosis that stabilizes joints and prevents further developing of deformities.

Post-poliomyelitis deformity, is an example of lower motor neuron lesion caused by a viral infection that attacks motor neurons in the spinal cord causing paralysis and atrophy. The degree of flaccid paralysis depends on the level of spinal cord involved.

Periphereal nerve injuries due to trauma, neuritis, or prolapsed invertebral disc cause several deformities and weakness in the part of the body innervated by the affected nerve. The principal obvious characteristic of patients suffering from peripheral nerve injuries is, thus, the flaccid nature of muscles. Treatments may involve orthoses that can hold the affected limb to improve muscle function. In particular if the peroneal nerve is affected there is loss of capacity to lift the foot and toes (dorsiflexion), as well as loss of the ability to evert the foot. The patient while walking drags the foot on the ground when bringing it forward. An ankle-foot orthosis is usually recommended when pereoneal nerve lesion occur.

Another disorder of the central nervous system is multiple sclerosis. The latter is a degenerative disease which destroys the myelin sheaths of neurons, leading to slowed impulse conduction or total block, and thereby nerve signals transmission between the brain, the spinal cord and other part of the body is impaired. Gait problems in patients affected by multiple sclerosis are related to muscle weakness, loss of coordination, sensory deficit, loss of balance, fatigue and spasticity. Those problems can be helped to some extent by physical therapy or ambulatory aids such as canes, forearm crutches, ankle-foot orthosis, and wheelchair in most severe cases.

2.2.2 Cerebral vascular lesions

Cerebral vascular accidents (CVA), also known as strokes, result from a loss of brain functions due to problems in the blood supply. Ischaemia of the brain can be caused by embolism, thrombosis, haemorrhage, atherosclerosis of the cerebral arteries, brain tumor and ruptured vascular aneurysm. As a result of a stroke, synergies at limbs often occur with hemiplegia, subsequent to a CVA, being one of the most common encountered causes of control dysfunction. Coordination of flexion and extension required for normal limbs movement is impaired with the resulting gait pattern depending on the extent of the lesion. One of the most common abnormalities seen in hemiplegic patients is equino-varus deformity, due to dorsiflexors and pronators weakness causing clearance problem during swing phase. Treatments include the use of orthoses, especially AFOs, or knee-ankle-foot orthoses (KAFOs) (Figure 2.2), for more severe cases.

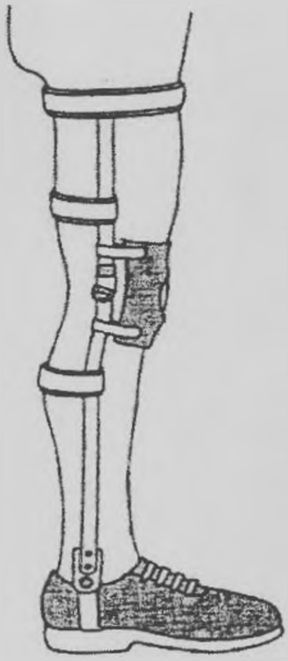

Figure 2.2: Metal and leather KAFO (AAOS, 1952).

2.2.3 Congenital Abnormalities

A congenital abnormality is a condition which is present at the time of birth which varies from the normal condition. It can be caused by genetic defects and environmental influences, or a combination of the two. Congenital talipes equino-varus is caused by an abnormal muscle development which distorts growing bones and joints causing a foot to be inverted and medially rotated. Prompt treatment with an AFO in infancy may reduced the deformity.

Spina bifida, is the most common congenital abnormalities of the spine, resulting from the failure of the vertebral laminae to unite during development. The pattern of motor dysfunction depends on the level and the extent of the spinal lesion. Orthoses may compensate for the resulting functional disorder.

2.2.4 Muscular Dystrophies

Muscular dystrophies are a varied collection of inherited diseases that produce progressive muscle weakness and deterioration. Principal symptoms include progressive muscular weakness, poor balance, walking difficulties, frequent falls and muscle contractures. There is no specific cure for these diseases, but orthotic management may assist patients during ambulation postponing complete dependence on wheelchair.

2.3 BIOMECHANICS AND FUNCTIONS OF LOWER LIMB ORTHOSES

Whether when standing or during dynamic activities, the body is subjected to external forces and moments in all the three orthogonal directions. In a healthy body, these external forces and moments are counteracted by the action of muscles, ligaments, or other normal body tissues.

As previously discussed a wide spectrum of diseases may compromise the ability of human tissues to resist or control external loads resulting in an abnormal pattern of motion. An orthosis applied to a patient can compensate for inadequate internal force system ensuring a safer and more natural gait pattern when lower limb impairments are involved.

There are four different ways in which an orthosis may modify the system of external forces and moments acting across a joint to restore more normal functions (Bowker et al., 1993).

First, an orthosis may modify the moments acting about a joint reducing the rotational joint motion, secondly it may modify the normal forces acting about a joint and thereby restrict translational joint motion at the joint. An orthosis, thirdly, may also provide an alternative pathway for the transmission of the applied load, reducing forces and moments carried across the joint. These three mechanisms are referred to as the direct action of the orthosis, by means the orthosis acts over the joint it encompasses. The fourth effect provided by an orthosis is the control of the line of action of ground reaction force (GRF). This mechanism is used mainly to modify moment about a joint or change the alignment of a joint. Realignment of GRF produces effects at all level of the lower limb, thus, this fourth approach is referred to as the indirect action of the orthosis.

Each mechanism described requires three forces to be applied on the patient's diseased lower limb segment. Pads, straps, hinged joint centres, elastic bands, springs or motor element may assist an orthosis in the treatment of pathological conditions.

The orthosis, finally prescribed, is strictly related to the particular functional deficit experienced by the patient and to the expected therapeutic outcomes. However four different classes can be defined in terms of orthoses in according to the major function provided: *supportive, functional*, *corrective*, *protective* othoses.
The largest class comprehends supportive orthoses used in treatments of all sort of conditions that require motor-control. Namely spasticity, flaccidity, painful joints, nerve deficits, architectural anomalies, trauma and congenital conditions can be treated with supportive orthosis. The latter aims to control joint motion, limit and prevent development of deformity.
Functional orthoses are characterised by mechanical joints, hydraulic cylinders, springs, elastic bands to impart active function. They are prescribed to compensate for weakened or absent muscle power. They are, primarly, used in the treatement of flaccid conditions.
To correct or realign parts of a limb, corrective orthoses are commonly used. They can be considered surgical tools, rarely used outside infancy.
Finally, protective orthoses, offer protection and maintain alignment for a painful joint.

An optimal design of an orthosis results from an evaluation of patient's condition along with the principles of design related to fuction of the orthosis.
With this regard an adequate load carrying area should be provided for comfortable pressure distribution. This aims to minimize the discomfort or damage to soft tissues, since an orthosis may apply quite considerable forces to the body. Joint positioning important for a better comfort, cost, ease of application, cosmesis, maintenance and weight should be also considered during orthosis design. Few of those characteristics may be controlled by the choice of materials used in orthotics fabrication. Materials used for the manufacture of orthoses will be discussed with particular reference to AFO manufacturing, in the next chapter.
Not less important is the knowledge of force interactions between the limb and the orthosis. The measurement of forces and moments applied by the external device is the objective of several studies with the aim to improve orthosis performance. Evaluation of loads applied by AFO on patients' leg during swing and stance phase of a gait cycle will be discussed in the following chapter.

CHAPTER 3

ANKLE-FOOT ORTHOSES

3.1 INTRODUCTION

The combination of the foot, ankle and associated musculature provides four major functions during gait:

1. provide a base of support to maintain an upright position without undue muscular effort;
2. provide a mechanism for the shock absorption of rotation of the limb segments above it during the stance phase of gait;
3. provide for the absorption of body weight shock at heel strike and provide for accommodation of uneven terrain;
4. act as a lever during push-off. (Leone, 1987)

As discussed in the previous chapter a number of diseases may interfere with the above-mentioned functions requiring the prescription of an ankle-foot orthosis (AFO) to minimize or correct the resulting gait abnormalities.

An ankle-foot orthosis, in fact, is an assistive device that is used to maintain ankle joint stability in the anterior-posterior and medio-lateral directions and also to permit and stabilize motion at the subtalar joint (Lehmann, 1979).Therefore an AFO is prescribed to assist a patient during ambulation supporting the lower leg and controlling the movement about the ankle joint by applying forces and moments to the patient's calf and foot.

Many designs of AFO have become available providing an orthotist with a range of devices, characterised by a different shape or material, that allow solutions to a large number of encountered lower limb disorders. The development of new designs is mainly related to the introduction of a wide variety of materials used in AFO manufacturing. Recently, in fact, the traditional AFO made of metal and leather has been largely superseded by plastic devices. A discussion about materials used for AFOs fabrication and advantages and disvantages of the use of conventional AFO or more modern plastic device is given in this chapter.

A description of the most common pathologies which are amenable to treatment with AFO will be given to the reader along with the appropriate ankle-foot orthosis prescribed in each case. Forces and moments action patterns applied by those AFOs on the patient's lower leg are also shown.
Although different lower limb impairments may be treated with different types of AFOs there are three basic considerations in prescribing an ankle-foot orthosis:

1. one should bear in mind that the orthosis is worn by a patient that can walk without it although not safely. To ensure safety the orthosis must provide adequate medio-lateral stability during stance phase;
2. the orthosis must provide adequate toe pick up during the swing phase;
3. it is desirable to approximate the normal gait pattern as nearly as possible and thus reduce energy expenditure (Lehmann, 1979).

A brief overview of studies conducted to evaluate the mechanics of this device will be also presented with particular attention to the load measurement system used. An understanding of AFO mechanics, in fact, is important to improve AFO designs and consequently its performances.
AFO performances can be investigated throughout a gait analysis of a subject wearing the experimental orthosis. A brief introduction on this technique is detailed in the present chapter. The terminology used in gait analysis is also explained so that the reader can better understand all the recalls made on human gait when dealing with pathologies that affect patients' locomotor system.

3.2 MATERIALS FOR AFO MANUFACTURE AND CORRELATED TYPE OF ORTHOSIS.

The design and the construction of AFO have undergone significant changes over the past few years due to the introduction of modern materials and technology. Historically orthoses were made from wood resulting in heavy and marginal efficacy devices. Improvement in orthosis fabrication was recorded in the '50s when stainless steel became the most preferred material by orthotist due to its strength, durability, and adaptability (Chu, 2001). Although it has less strength to withstand body weight, in 1960 aluminium first appeared in orthopaedic industry. To those periods belong the so called conventional AFO based on metal and leather components.

A conventional AFO, still in use nowadays, is characterised by double uprights made of steel or aluminium alloy (Figure 3.1).

Figure 3.1: Conventional metal and leather AFO with double uprights (McHugh, 1987).

However, a single bar design, with the upright located posteriorly, medially, or laterally to the ankle joint, may be sufficient to treat less severe lower leg disorders. The uprights are attached proximally to a leather calf band, and distally they are usually connected to an ankle joint mechanism. The latter, in turn, is permanently anchored to the shoe or to foot attachments allowing shoe interchangeability. Different types of ankle joint mechanisms are available, although a single axis design, which prevents medio-lateral motion, is usually fitted on the patient's orthosis. The unique conventional design that does not incorporate mechanical joint is the wire spring AFO (Figure 3.2).

Figure 3.2: Wire spring AFO (McHugh, 1987).

Conventional AFOs may also include springs, or additional straps at ankle level (e.g.: T-strap) to correct or compensate muscle impairments.

The biggest movement in the orthotic technology occurred in the late '70s when thermoplastic materials were adopted in the rehabilitation field (Chu, 2001). Since then, polypropylene has become the most widely used and accepted material for orthotic applications (Showers et al., 1985). It provides high fatigue resistance, high strength, light weight, excellent moulding properties and a better cosmesis compared to metal and leather AFO.

Figure 3.3: Polypropylene AFO.

Nowadays, in addition to polypropylene, other types of materials are being used in this field. The particular characteristics of each of those materials make them more suitable for certain disability treatments. The decision to use one type of plastic over another, however, is being determined more frequently by the orthotist (Showers et al., 1985).

The techniques applied to fabricate a plastic AFO require that a negative cast of the patient's lower limb segment be taken. Once the cast is set and removed it is filled with plaster of Paris to obtain a positive model of the patient's extremity (Figure 3.4). The positive model is rearranged or modified by the orthotist in order to provide the maximal orthotic fit and function. This step in AFO manufacture is critical. A plastic sheet is then draped over the cast and a custom-moulded AFO is thus obtained.

Figure 3.4: Patient's positive cast with trim line on it.

Plastic AFOs can be also prefabricated; mass produced orthoses in a variety of fixed sizes and in a variety of materials. Although they are cheaper than custom-moulded AFOs, they do not achieve the same accuracy of fit and function provided by custom- moulded AFOs. Some prefabricated AFO can be further modified by heating techniques to obtain as close a fit as possible. This method is called custom fitted and the orthoses are referred to be custom-fit orthoses. Although these orthoses are more functional, and provide better fitting compared to just prefabricated orthoses, they are still less likely to meet patient's need than custom-moulded orthoses.

The rigidity of a plastic AFO can be varied depending on the trim line on the patient's cast, the thickness of the plastic sheet used, and its chemical composition.

Polypropylene is the strongest and most common sheet plastic available which can be formed over a positive model (Showers et al., 1985). The posterior leaf spring AFO (Figure 3.5) is a common polypropylene AFO characterised by a narrow calf shell which provides this orthosis with a great flexibility.

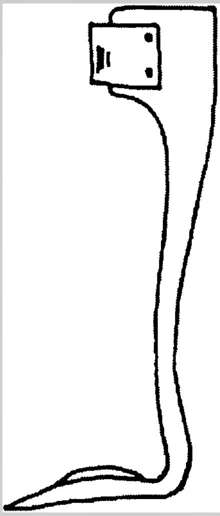

Figure 3.5: Posterior leaf spring AFO (Lim, 1985).

Solid AFOs (Figure 3.6) or Patellar Tendon-Bearing AFOs are also usually made from polypropylene.

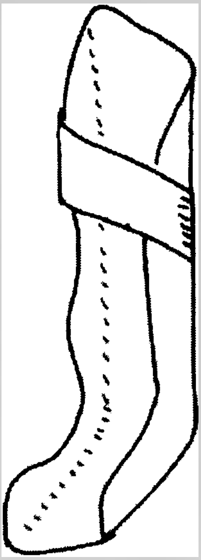

Figure 3.6: Solid AFO (Lim, 1985).

Polyethylene is the next to polypropylene in popularity with orthotists (Showers et al., 1985). Its cost effectiveness, flexibility, workability, and pleasant appearance make polyethylene a good alternative to polypropylene for AFO manufacture.

Ortholen, ultra high density polyethylene, is also used in AFOs fabrication. It is characterised by a good memory, resistance to corrosion and high flexibility.

The spiral and hemispiral AFOs are usually made of Nyoplex. It is cosmetic and transparent, but durability is still a problem in these applications (Showers et al., 1985).

A spiral AFO (Figure 3.7) consists of a spiral that originates from the foot plate twisting around the leg anteriorly and posteriorly and terminating laterally with a calf band.

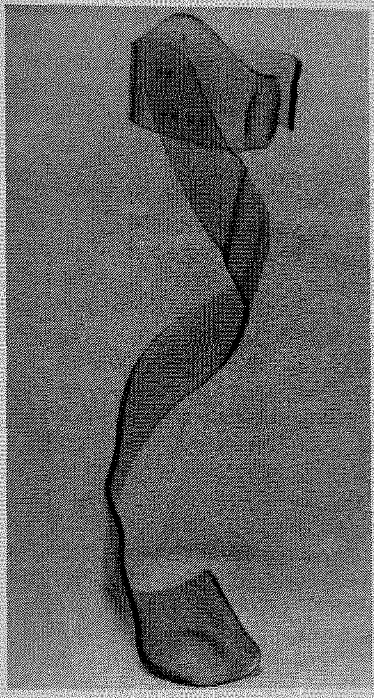

Figure 3.7: Spiral AFO (Bowker et al., 1993)

Hemispiral AFO, instead, only makes a half turn round the leg resulting in a less flexible device. The more obvious disadvantage for those orthoses that coil round the patient's leg is their difficulty to be donned and doffed.

Although when talking about plastic AFO, it is common to refer to one-piece plastic device, more recently AFOs, characterised by two plastic pieces hinged around an ankle joints, have been introduced. Functions provided by articulated AFO depend on the type of ankle joint and on how it is set.

Regardless of AFO specific design or the materials used, the ability of an AFO to achieve maximum benefit is greatly influenced by the shoe worn by the patient. Changing a shoe, in fact, can alter the biomechanical function of the orthosis.
Although thermoplastic designs are most often used, in some circumstances, a conventional AFO may be more appropriate. For example when changes in a patient's condition are expected an adjustable conventional AFO is preferable. Later, as the condition stabilizes, and adjustability is not required anymore, a plastic AFO may be fitted. Different factors should be evaluated for an appropriate AFO prescription including the degree of muscoskeletal impairment or deformity, hypertonicity, presence of motor control disorder, and the anticipated prognosis by means of evaluation of growth and progression of the disease process. An appropriate consideration of all these factors will result in a positive and beneficial orthotic outcome for the patient.
A brief overview of advantages and disadvantages of the two main categories of AFO, plastic and conventional, is given in the following paragraph.

3.2.1 Metal vs Plastic AFO

The more obvious advantage of plastic AFO is the improved cosmesis. Plastic AFOs can be easily hidden under clothes and shoes interchangeability is also allowed. Those factors contribute to greater orthosis acceptability by patients, breaking the stereotypes of disabilities set by society (Shamp, 1983).
The use of thermoplastic materials result also in lighter device thus reducing energy requirements during patients activities. They are relatively cheap to produce, can be manufactured quickly and require less maintenance than conventional orthoses (Bowker et al.,1993) In addition hygiene concerns are easily met with plastic orthoses that may be cleaned daily (Shamp, 1983)..
However the effectiveness of plastic AFO is dependent on the manufacture and fit of the orthosis itself. Continuous improvements should be made for a better orthosis quality. The development of new technologies, such as the computer assisted fabrication CAD/CAM methods, may allow more accurate orthoses construction improving their function once fitting on a patient's leg.

Although a higher quality of orthotic practice may be achieve with orthotist experience and further research, the problem of plastic AFOs adjustability still remain a disadvantage for those AFOs compared to the traditional metal and leather ones. Conventional AFOs adjustability is the main reason for the continued popularity of those devices, which can be easily set to accommodate growth or other patient's changes following orthotic treatment.

Either conventional AFOs or plastic AFOs base their function on a 3 point-force system applied on the patient's leg. The area upon which forces are applied is greater in plastic AFO reducing potential of high pressure, discomfort, and skin breakdown. Although the advantage of adjustability and the fact that their effectiveness is well recognized in clinical practice, the introduction of plastic materials have reduced the prescription of conventional AFOs since more advantages have been recognized to the use of plastic materials.

3.3 GAIT ANALYSIS

Walking is the body's natural means of moving from one location to another; it uses a repetitious sequence of limb motion to move the body forward while simultaneously maintaining stance stability (Perry, 1992).

Ambulation is a functional outcome of a complex interaction between neuromuscular and structural elements of the lower locomotor system. Its efficiency thus depends on central nervous system activity which coordinates motor and sensory units of the lower extremity, free joint motion, and muscle activity.

Alteration of muscle effectiveness and mobility will result in an abnormal gait pattern. Assessment of pathological conditions affecting locomotion necessitates gait analysis, defined as the set of methods and techniques aimed at quantitative analysis of human motion (Rose and Gamble, 2006). From the examination of the patient's walking ability, diagnosis of an abnormal gait is obtained and clinical decision can be made for an appropriate treatment. Gait analysis, in addition to clinical assessment, also represents an important instrument in the research field, either with a medical or engineering point of view.

A variety of gait analysis techniques, which differ in data provided, cost, quality of data, are used to study human gait. These range from observational gait analysis, in which no equipment is required to more sophisticated instrumented analysis based upon the use of technological devices that allow kinematic and kinetic analysis.
The purpose of this section is to give to the reader a brief overview of the gait cycle for a better understanding of the following paragraphs and subsequent section describing the gait analysis conducted. The instrumentation used for this purpose is, also, shortly detailed later on.

3.3.1 Gait events

A gait cycle, also known as stride, is defined as the time interval between two successive ipsilateral foot contacts. The time of two consecutive opposite foot contacts, instead, is called step, hence in each stride there are two steps (Figure 3.8).

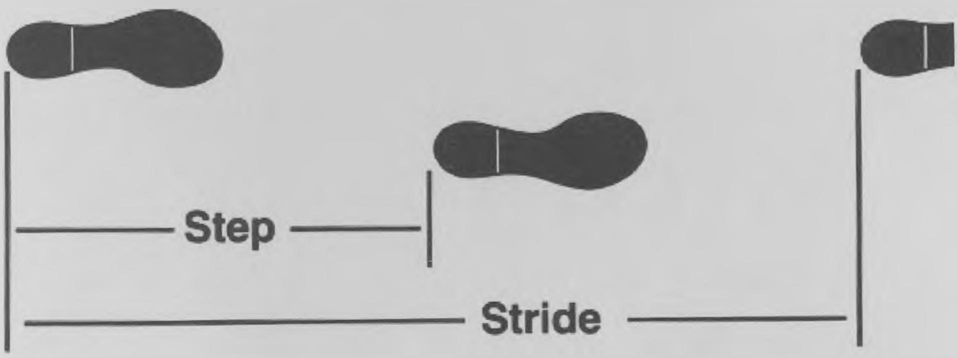

Figure 3.8: Difference between step and stride (Perry, 1992).

Each gait cycle is divided into two periods: stance and swing (Figure 3.9).

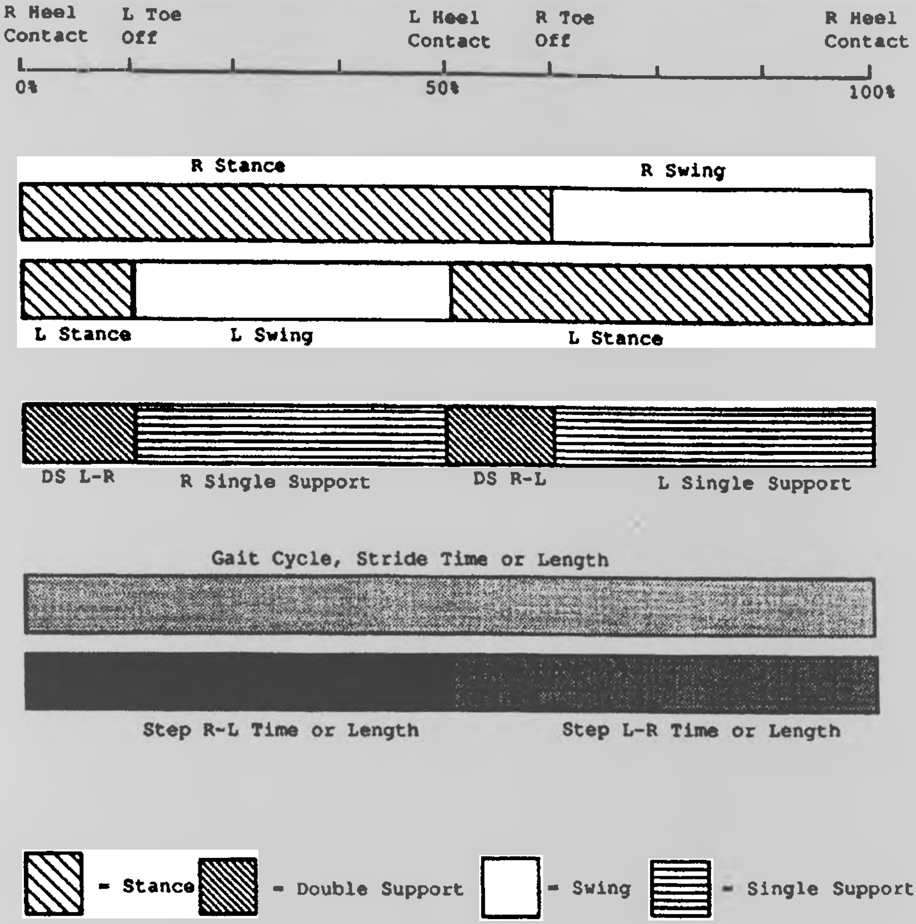

Figure 3.9: Temporal parameters of the gait cycle (Finney,1997).

The stance phase is the period of time during which the foot is in contact with the ground. It begins at heel strike (initial contact) and ends with toe off, encountering for approximately 60% of one gait cycle. Swing phase, which occupies the remainder 40% of the stride, is the time during which the foot is in the air. Swing begins at toe off and ends at the following initial contact when another gait cycle starts. During a gait cycle an alternation of a double and single support occurs, with each period of double support about 10% of the entire cycle. However, the precise duration of these gait intervals varies with the person's walking velocity, showing an inverse relationship to walking speed (Perry, 1992). The final disappearance of the double support phase marks the transition from walking to running. At the customary 80 m/min rate of walking the stance and swing periods represent 62% and 38% of the gait cycle respectively (Perry, 1992).

Stance and swing phase can be subdivided in smaller intervals, as shown in the figure 3.10 below, with anatomical positions of the foot being the identification points of those events.

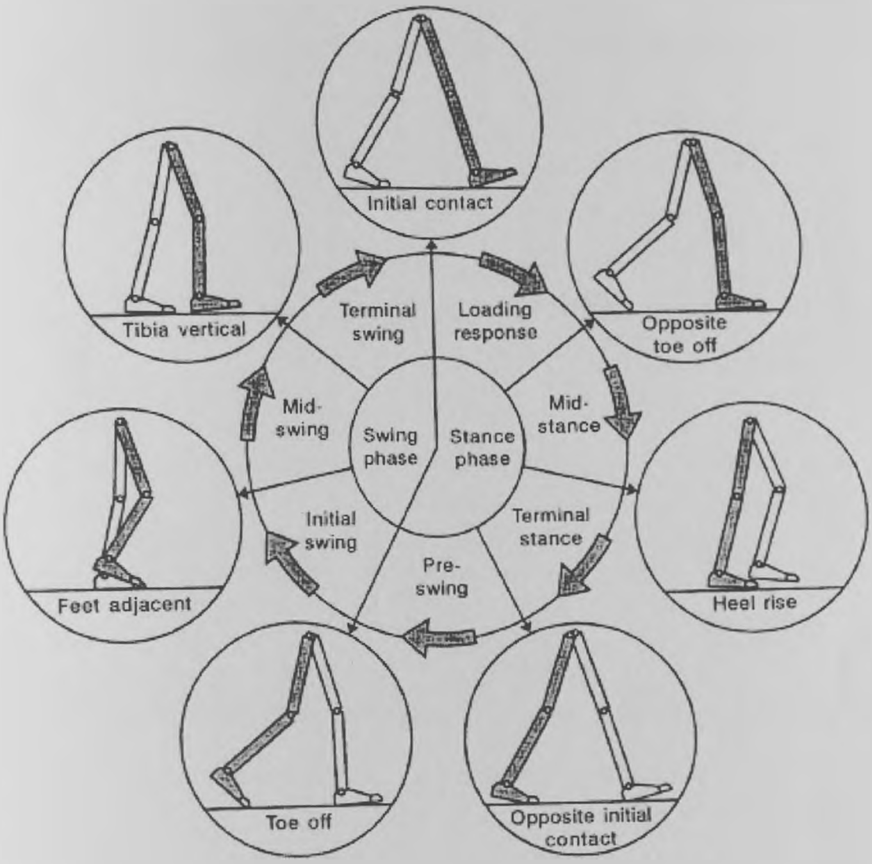

Figure 3.10: Gait cycle by the right leg (Whittle, 2007)

3.3.2 Gait parameters

Important parameters usually evaluate when performing gait analysis are joint angles, at the hip, knee and ankle, ground reaction forces, in the three dimensions and the related moments about the joints.

During gait movements occur in sagittal, transverse and frontal plane. For simplicity, as example, this brief introduction will concentrate only on the sagittal plane, in which the largest movements occur. For each of the mentioned parameter a constant pattern has been found when data of a normal subject were plotted against the percentage of a gait cycle. Those graphs provide a standard against which the gait of a patient can be judged.

Figures 3.11, 3.12 and 3.13 show sagittal plane angle at the ankle, knee, and hip joint. At initial contact ankle plantarflexs until foot flat is achieved (Figure 3.11). At this point ankle changes its direction toward dorsiflexion continuing to dorsiflex until it reaches a maximum peak of around 10° in dorsiflexion. A rapid plantarflexion follows to a maximum of 20-25° just as the foot is pushed off the ground. During swing phase the ankle moves back into dorsiflexion until it reaches a neutral position maintained for the rest of the cycle. Muscles, involved in the ankle joint movements, are mainly plantaflexors and dorsiflexors active respectively in stance and swing phase.

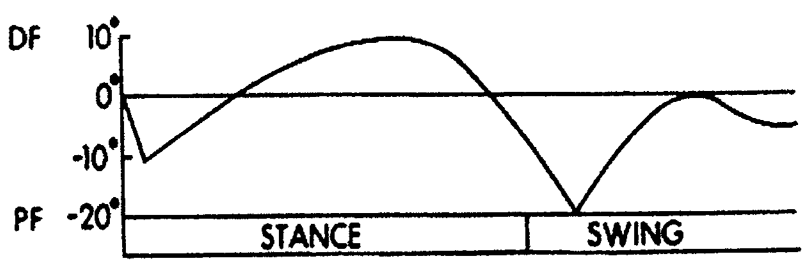

Figure 3.11: Ankle angle during a gait cycle. DF and PF stand for dorsiflexion and plantarflexion (AAOS, 1985).

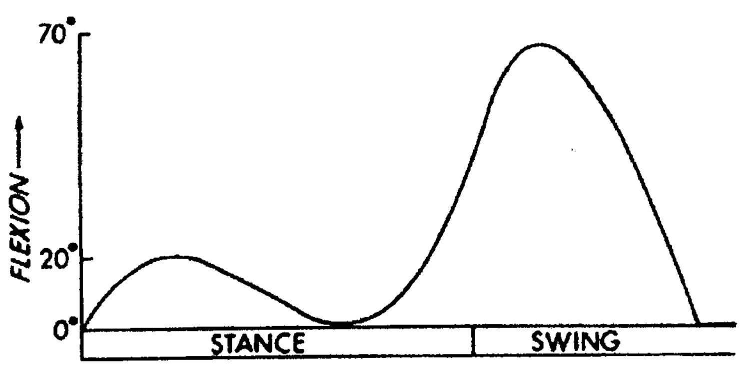

Figure 3.12: Knee angle during a gait cycle. (AAOS, 1985).

The knee has two flexion waves each starting in relative extension (Figure 3.12). The first wave allows shock absorption and is due to the action of quadriceps muscles. The second flexion wave begins at heel off reaching a peak during initial swing of 60° that is the maximum knee angle occurring during the gait cycle (Perry, 1992). The limb, thus shortens allowing ground clearance. The knee, finally, extends again before a new cycle starts.

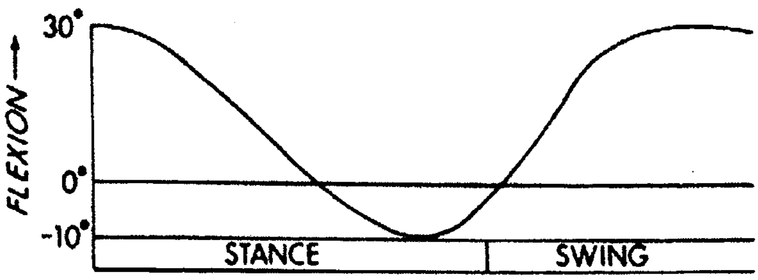

Figure 3.13: Hip angle during a gait cycle. (AAOS, 1985).

At heel strike the hip is flexed and extends until the end of stance phase when it starts to flex again until the following initial contact (Figure 3.13). The peak in extension is about 10°, whereas the limit of flexion is 35° (Perry, 1992). The main muscles involved are the hamstrings, iliacus, rectus femoring and gluteus maximus.

The ground reaction forces (GRFs) are external forces acting on the body that are equals in magnitude but opposite in direction to those being experienced by the body. They are related to both gravitational acceleration and mass acceleration due to body weight movement from one limb to another during each gait cycle (Perry, 1992). Forces plates accomplish the measurement of GRFs, eventually in all the three orthogonal directions: vertical, medio-lateral, and antero-posterior components of the GRF can be measured. When those components, usually expressed in terms of body weight, are plotted against the percentage of gait cycle typical patterns emerge when dealing with normal subject.

The vertical force shows a characteristic double hump in which the force oscillates between approximately 110% and 80% of the body weight (Figure 3.14). Peak related to a GRF greater than body weight is due to a body's positive acceleration in the vertical direction, in other words, an upward movement f the body centre of mass (COM). A downward acceleration of the body COM, by contrary, causes a GRF to drop below the body weight.

Anterior-posterior forces result from friction between the foot and the ground reflecting the forward and backward acceleration of the body. The maximum horizontal forces reached are typically around 20% of the body weight (Figure 3.14). Magnitudes of medio-lateral forces are generally very small, 5% of the body weight (Figure 3.14), reflecting small acceleration in the medio-lateral direction due to the exchange of body weight from one limb to the other.

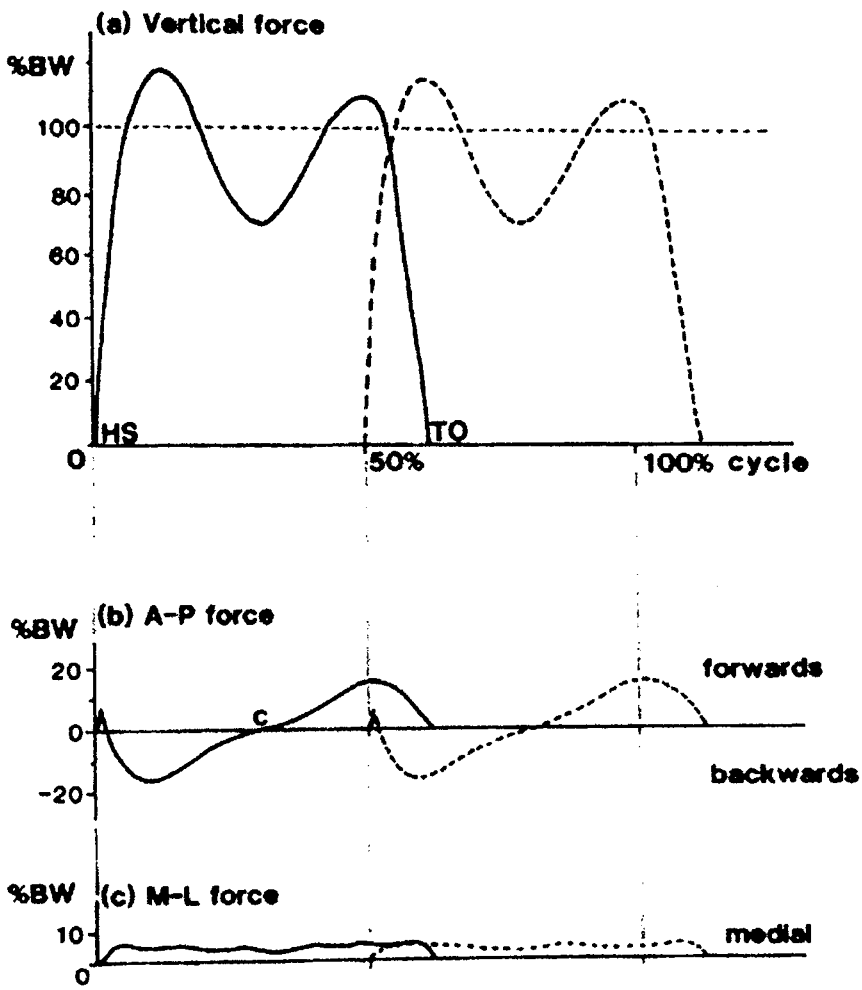

Figure 3.14: The three components of the GRF acting on the foot during a gait cycle. (Finney, 1997).

A moment is defined the product of the force and its lever arm. In gait analysis the force is represented by the GRF ant the lever arm is the perpendicular distance between the force line of action and the joint. The moment defined by the product of those values is referred to be an external moment which will be resisted by the muscle action creating an internal moment (Figure 3.15). When calculating moments the effects of gravity and inertia are not included (Perry, 1992). Sagittal plane data defined a flexion or extension moment in according to the position of the GRF respect to the joint.

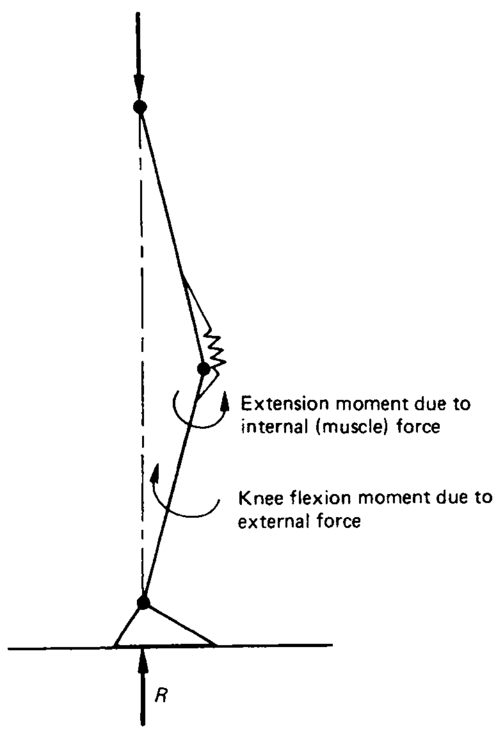

Figure 3.15: Moment exerts by the GRF is opposed by the muscle activity (stance phase) (Bowker et al., 1993).

3.3.3 Example of method used in gait analysis

A system of forceplates, disguised on a laboratory floor, is usually used to measure ground reaction forces and moments in three orthogonal directions. Commonly a forceplate has an upper surface area measuring 40x60 cm and four transducers, one in each corner. Each transducer generates a signal in response to a mechanical deformation due to patient walking across the platform. These signals are converted into voltages by a series of amplifiers and recorded by a PC using particular software created for this purpose. In the gait laboratory of the Bioengineering centre a VICON 370 system is available.

Infrared cameras are positioned on tripods in the gait laboratory around the forceplates for kinematic data acquisition. Markers placed on patient's limb reflect the infrared light emitted by the cameras allowing the latter to capture subsequent frames of body segments in 3 dimensions. Each camera is usually linked via an etherbox to a computer where images can be viewed on the screen and kinematic data recorder. To achieve reasonable accuracy in kinematic measurement, it is necessary to calibrate the cameras prior data collection. Calibration allows the automatic calculations of positions and orientations of the cameras relative to each other and to an origin and set of axes. Cameras are first positioned ensuring a clear view of the capture volume; following, a static and dynamic calibration is performed running a calibration program usually part of the software installed in the laboratory computer for gait analysis (e.g.: VICON 370 software) . An L-frame (Figure 3.16) with markers attached on it, located on the edge of a forceplate, is used for static calibration to determine the origin of the orthogonal axes whereas a wand with two markers on it is waved throughout the capture volume for the dynamic calibration.

Figure 3.16: L-frame and wand used for cameras calibration.

Upon completion of a successful calibration, cameras parameters are automatically stored. Cameras must remain in the same position for the duration of the tests.

After calibration the capture volume successfully, it is possible to move towards the preparation of the subject. Markers are attached to key point identifying the underlying skeleton. These skin markers, however, do not provide the accurate anatomical landmarks position due to soft tissue movement around bony segments. For this purpose an anatomical calibration procedure is carried out, mostly following the method described by Cappozzo et al. (1995). During calibration, the subject is positioned in its normal standing posture, in full view of all cameras and a wand with two markers is used to point the anatomical bony landmarks (Figure 3.17) while their positions are captured for a period of around 1 second.

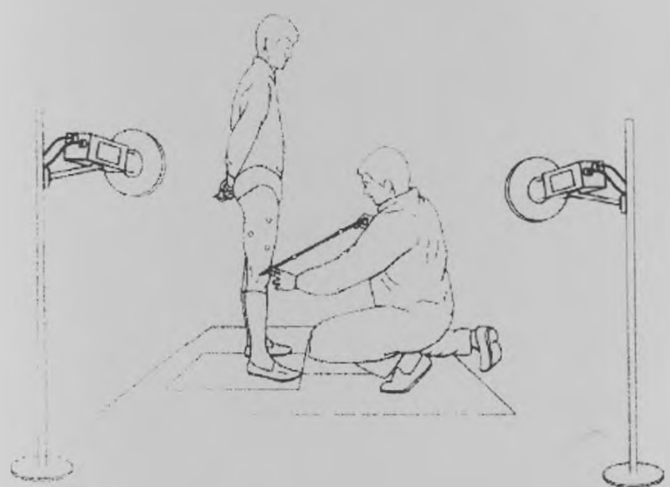

Figure 3.17: Calibration of the subject using the pointer (Cappozzo et al.,1995).

The 3-D coordinates of the anatomical target point could be estimated knowing the length of the calibration stick and the distance between the two markers. When this procedure is completed the motion capture of the subject can be carried out. The subject is asked to walk across the gait laboratory without focusing on stepping on the forceplatforms in order to avoid an artificial gait pattern. Typically the subject has to walk several times before obtaining good data showing a whole footstep of the limb on a forceplate. Data from the camera and forceplates are recorded on the computer of the laboratory. Information recorded can be processed using appropriate software package for gait analysis combined with Microsoft Excel spreadsheets.

What has been described is a common methodology used for gait assessment; other possibilities are available in according to the aim of the studies. Patients can perform different tasks than just walking and be tested while wearing an instrumented orthosis to study the performance of the latter.

3.4 PRINCIPAL PATHOLOGIES

Various locomotor disorders may be treated with an AFO. They refer to:

- conditions which result in weakness of the muscles which control the ankle-foot complex (motor disorders)
- upper motor neuron lesions which result in hypertonicity and spasticity of the muscles
- conditions which result in pain or instability due to loss of integrity of the lower leg ankle –foot complex (Bowker et al.,1993).

3.4.1 Motor Disorders

Muscle weakness is usually encountered as a result of injury to a nerve or tendon, prolapsed intevertebral disc, sacral neurological lesion, and lower motor neuron diseases. The objective of AFO for this category of functional deficit is to replace the function of the weakened muscle. Most commonly affected muscles at the lower leg level are dorsiflexors, plantaflexors, pronators and supinators.

a. Weak or absent dorsiflexors

During the stance phase of gait the dorsiflexors are involved both in the control of initial plantarflexion and in the pulling of the body weight over the supporting foot. During swing phase on the other hand, they ensure a sufficient clearance of the foot over the ground, dorsiflexing the foot. In pathological conditions derived from weakness of dorsiflexor muscles the moment created by the weight of the foot is unopposed, thus leading to a rapid plantarflexion in early stance ending with a foot slap, and to drop foot which imperil ground clearance during swing phase.

Orthotic management for this disorder requires a three-force system positioned to resist plantarflexion at heel strike, preventing foot slap, and to support the foot during swing phase preventing drop foot.

Forces applied on the lower leg by AFOs either at heel contact or swing phase are shown in figure 3.18.

Conventional orthoses seek to compensate for weakened dorsiflexors by virtue of the forces generated on the calf band attached at the proximal end of the two metal uprights, and on the upper and sole of the shoe. Conventionally constructed orthoses for these purposes incorporate a mechanical ankle joint and a spring, acting about the joint, to resist plantarflexion.

A more current treatment for weak dorsiflexors is provided by plastic posterior leaf spring orthoses (Figure 3.5) , usually made from ortholen. The three forces required are achieved through the contact of the calf section and the foot piece of the orthosis acting in concert with the shoe upper (Bowker et al.,1993).

Ankle joint control is achieved by virtue of the flexibility/stiffness of the posterior wall of the orthosis.

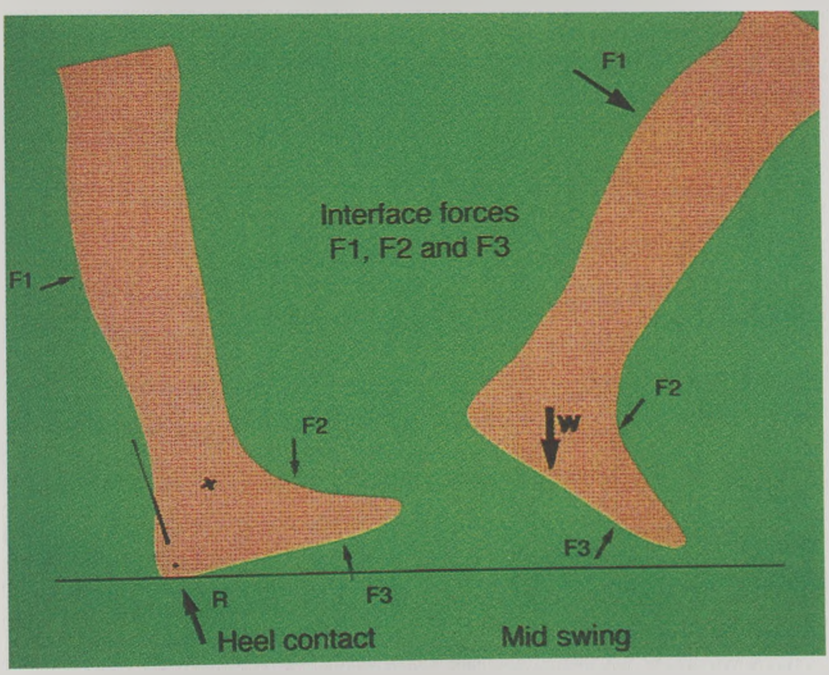

Figure 3.18: Three-force system required in absence or weakness of dorsiflexors at heel contact and midswing (Condie and Turner, 1997).

b. Weak or absent plantarflexors

Weakness of the plantarflexors results in excessive dorsiflexion and loss of push off, reducing walking speed and efficiency during stance phase.

The orthotic requirement is to provide a three-force system to resist the external dorsiflexion moment induced by the ground reaction force as illustrated in figure 3.19.

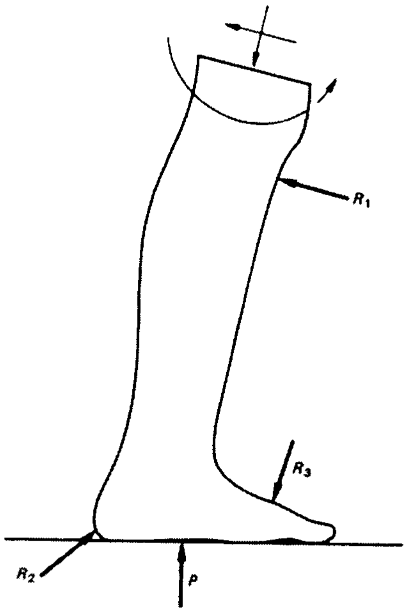

Figure 3.19: Three-force system required to control excessive dorsiflexion (Bowker et al., 1993).

Conventional orthoses with incorporation of ankle-joint design to limit dorsiflexion may be used for this purpose, or alternatively the plastic Floor Reaction Orthosis. The latter shown in figure 3.20, has the disadvantage of being a rigid construction that also prevents plantarflexion. The addition of an ankle joint which permit plantarflexion but prevent dorsiflexion may address these requirements (Condie and Turner, 1997).

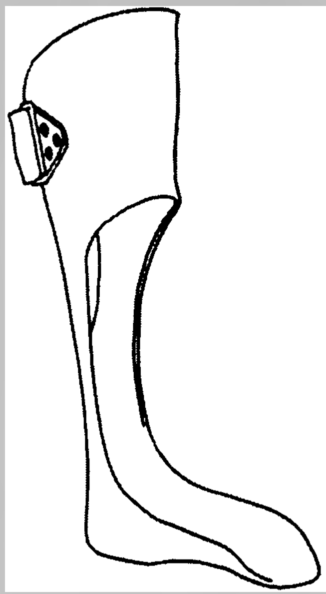

Figure 3.20: Floor reaction orthosis.

c. *Weak or absent pronators or supinators*

Weakness of pronators will result in a varus position of the foot during swing phase, whereas weakness of supinators will result in a valgus position of the foot during weight-bearing (Figure 3.21).

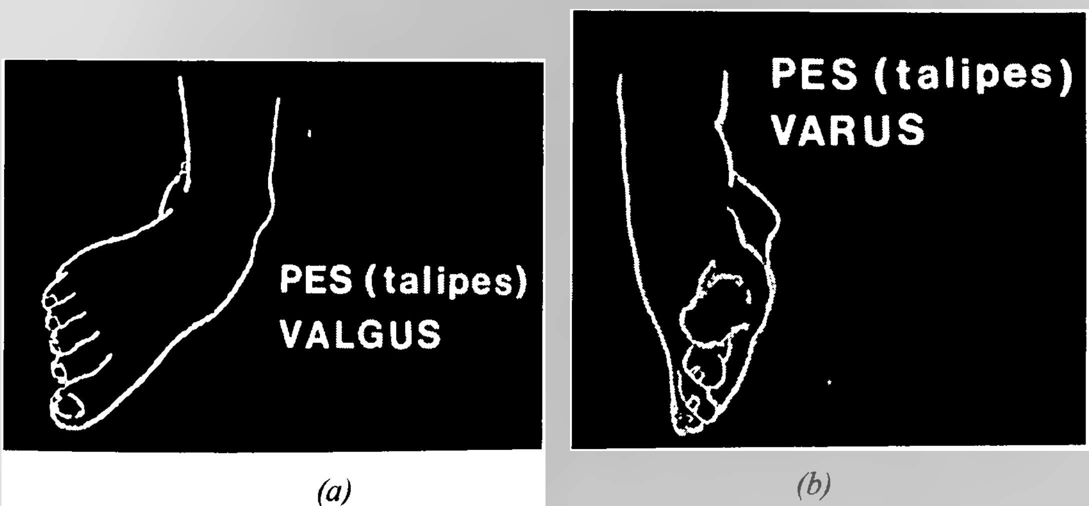

Figure 3.21: Valgus (a) and varus (b) position of the foot.

Patients affected by pronators or supinators weakness may also present weakness of dorsiflexors or plantarflexors therefore orthotic requirements for those patients will

be characterised by the same features necessary to compensate for the disorders described above with additional feature to control varus or valgus instability.
The three-force system required to correct varus and valgus is illustrated below (Figure 3.22).

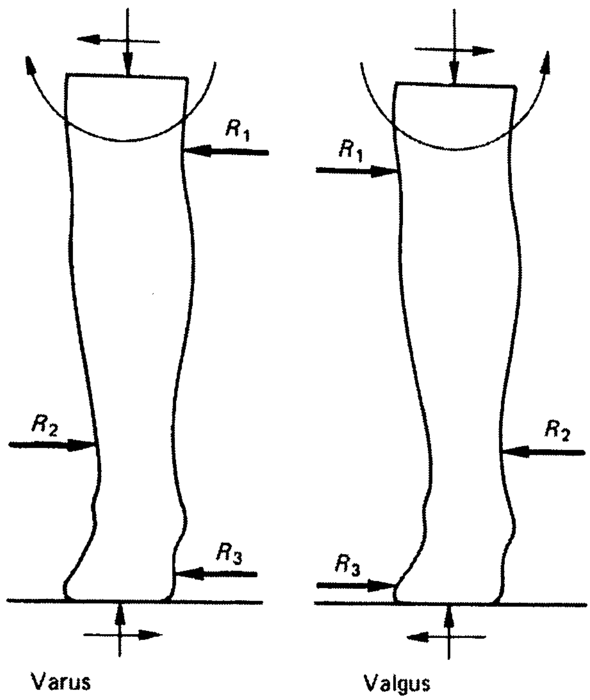

Figure 3.22: Three-force system required to control varus and valgus (Bowker et al., 1993).

This system can be either provided by a conventional orthosis, or polypropylene AFO or by spiral ankle foot orthosis. The conventional orthotic treatment consist in a double metal bar orthosis with a proximal calf band which provides the upper force shown in the figure 3.22, and a T-strap positioned medially or laterally respectively to resist pronation and supination which provide the central force (Figure 3.23). The third force is provided by the shoe. This orthosis incorporates also an ankle-joint which controls ankle motion.

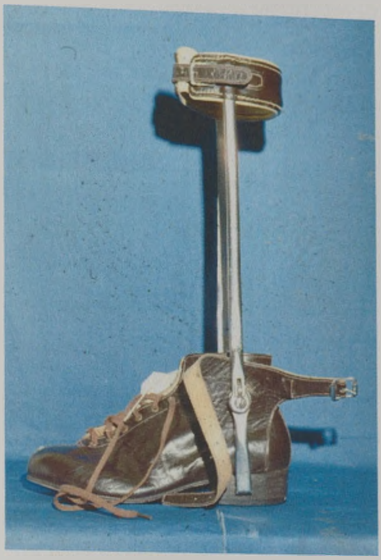

Figure 3.23: Conventional AFO with a T-strap.

In the Polypropylene AFO the force system is obtained by contact between the orthosis and the lower leg. The trimline of the AFO may be adjusted to provide the required degree of control.

The spiral ankle foot orthosis seeks to achieve the requirements to correct varus and valgus by applying a four-force system. The latter is characterised by two force couple generated between the moulded calf band and the leg and the footpiece-shoe combination and the foot (Bowker et al., 1993). Forces applied by a spiral type AFO are shown in figure 3.24.

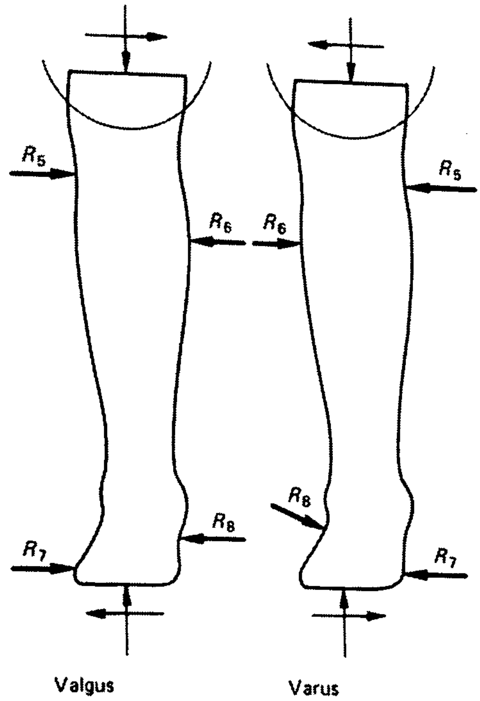

Figure 3.24: Four-force system applied by a spiral AFO to correct valgus and varus (Bowker et al., 1993).

3.4.2 Upper motor neuron lesions

Upper motor neuron lesions, arisen from cerebral palsy, multiple sclerosis, head injury, and cerebrovascular accidents will result in abnormal muscle tone, known as spasticity. AFO used in the management of these pathological conditions have to resist internal abnormal moments generated by the high muscle tone.

Equinus and equninovarus position of the foot are the most common problems following upper motor neuron disorders.

a. Equinus

Equinus position of the foot will result from an increased tone in the plantarflexor muscles. Typically no heel contact will occur. Treatment is based on the use of AFOs that must resist plantarflexion by applying a three-force system (Figure 3.25).

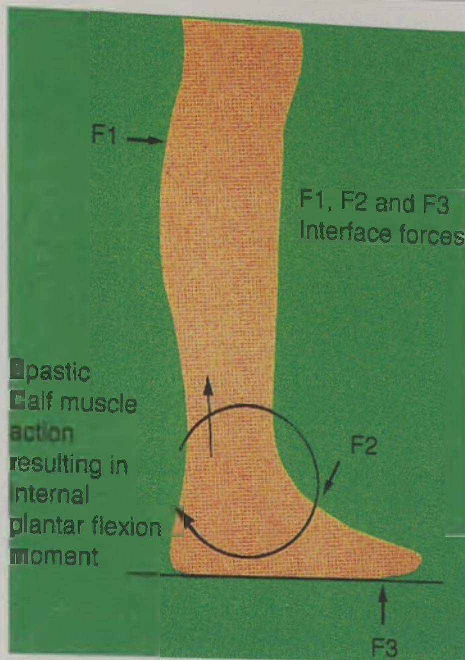

Figure 3.25: Three-force system to control equinus position of the foot (Condie and Turner, 1997).

A conventional AFO with two metal bars and an appropriate ankle joint may be fitted in patients who manifestate equinus position of the foot, or alternatively, a rigid polypropylene AFO may be prescribed. An ankle strap will prevent the foot to rise out of the plastic orthosis. A different approach may be the prescription of an articulated AFO which will allow passive dorsiflexion while resisting plantarflexion (Bowker et al., 1993).

b. Equinovarus

Equinovarus position of the foot is a manifestation of cerebral injury which leads to clearance problems during swing phase. Initial ground contact will be with the toes and lateral border of the foot. The force system applied should resist both plantarflexion and supination (Figure 3.26).

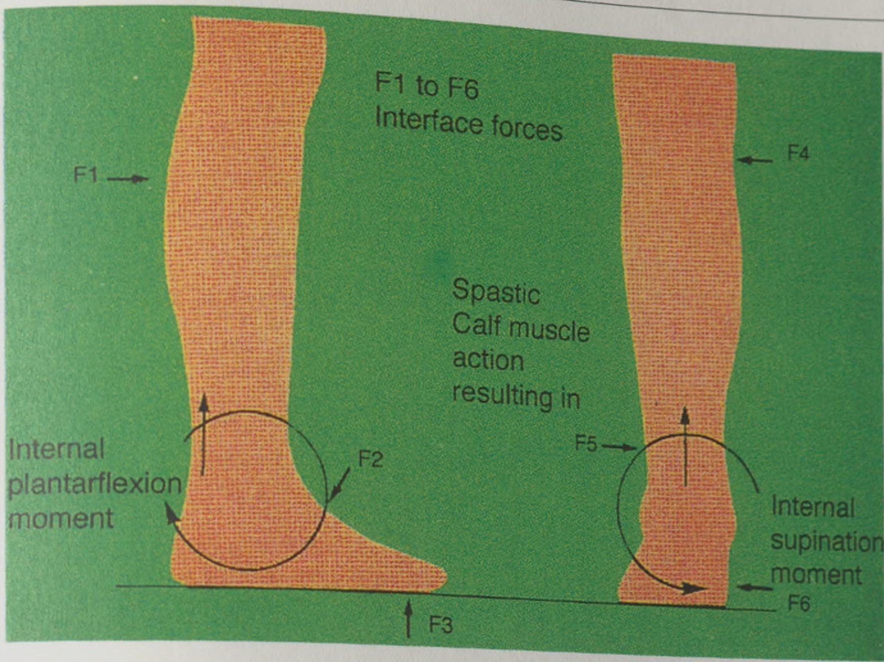

Figure 3.26: Two three-force systems to resist plantarflexion and supination applied to correct equinovarus deformity (Condie and Turner, 1997).

A conventional AFO with a T-strap located over the lateral malleolus to correct supination and an ankle joint which resist plantarflexion may be used to treat equinovarus. The advantage of this AFO over a plastic one is the compliance of the leather against the leg which should ensure comfort and potential for adjusting the amount of correction upon the joint (Bowker et al., 1993).

3.4.3 Impaired structural integrity

Structural disorders are commonly caused by trauma or arthritic conditions. The principal consequence to those conditions is pain following ankle motions. The AFO will therefore provide pain relief and compensate for the resulting limitations of the normal joint function. If pain is experienced on weight bearing a solution might be provided by patellar tendon bearing AFO.

3.5 REVIEWS OF ORTHOTIC LOAD MEASUREMENT SYSTEMS

The biomechanical assessment of an orthotic device is essentially a quantitative analysis of the biomechanical function and mechanical characteristic of the device.

To study the biomechanical function of an orthotic device, subjects are fitted with the experimental orthosis to allow measurements to be taken during a gait cycle. In order to achieve this purpose the orthosis will be properly instrumented to record orthotic loads. Commonly measurements are performed in a gait laboratory having force plates and camera system using optical markers.

Mechanical evaluation, instead, can be achieved from loading tests performed on the orthosis itself.

A search of the literature revealed that only few computational and experimental studies have been conducted into the biomechanics of the AFOs. Experimental testing researches are briefly reviewed.

3.5.1 AFO loading investigations

Magora et al. (1968) described a technique for the evaluation of strains evolved in conventional drop-foot AFOs with the aim to ascertain the loads applied to the orthosis. Brace fatigue and fragility in fact may compromise performances of the AFOs. Miniature strain gages were attached to the duraluminium stirrup beneath the ankle joint, with four strain gauges been used on each side of the brace. The experiments were conducted on three healthy subjects, who performed different types of gait at request. Results from this study revealed variations in the strains evolved in the conventional AFO varying the gait pattern and the position of the foot. The highest strain was found in the outer uprights and a total axial force that exceeded the weight of the subject was recorded during gait in forced inversion (Magora et al., 1968).

To explain the individual variations shown in the aforementioned work Robin et al. (1968) investigated seven different types of AFOs designed to correct drop foot on a single normal subject.

The highest stress was recorded in posterior spring AFOs, where it reached a value of 257 MPa, whereas values recorded in bilateral uprights AFOs were much smaller. The lateral bar showed a higher stresses compared to its medial counterpart.

Robin and Magora (1969) conducted a stress analysis on conventional AFOs fitted in four patients suffering from drop foot due to paralysis of the dorsiflexor muscles following poliomyelitis. The comparison of results from drop-foot suffering patients with results from normal subjects showed that loads in the direction of gait were similar, whereas loads in lateral direction were approximately double in patients with a paralysed limb. The maximum stress in the current study was recorded during stance phase and it was found to be double of those obtained on healthy subjects. This stress might be reduced, in according to the conclusion of the current study, designing an AFO that operate to prevent drop foot only during swing phase.

Lehman et al. (1983) evaluated five different types of plastic AFOs as to the amount of plantarflexion-dorsiflexion resistance provided in hemiplegic patients and normal subjects. A goniometer was used to measure ankle angle, whereas gait occurrences were recorded by a gait event marker. This study highlights the different performances of AFOs in terms of flexibility during heel strike, swing phase and push off, providing information on the behaviour of various plastic AFO designs, and in turn making them more suitable for certain clinical conditions.

Different research projects have been focused in the effects of AFO on patients' walking pattern. Just to mention few works: Dieli et al. (1997) investigated the effects of the dynamic AFO (DAFO) on three post-cerebrovascular accidents hemiplegic patients. With VA-Rancho Stride Analyzer, a computerized system for collecting and analyzing data via sole footswitches, they measured and analyzed the stride characteristics, including walking velocity, stride length, cadence, stance time, swing time and single-limb support. The results of this study have demonstrated the positive effect of dynamic AFOs on the gait of hemiplegic adults when compared to the barefoot and prefabricated-AFOs. In particular the results displayed an increase in walking velocity, stride length, cadence and single-limb support on the affected side when using the DAFO justifying the more common actual use of dynamic orthoses.

Mc Hugh et al. (1999) investigated the magnitude and orientations of the force actions between the AFO and the lower leg encompassed by the orthosis in conditions of dorsiflexor and plantar flexion insufficiency. It has been reported that forces required to compensate for lack of plantarflexion in late stance phase are greater than forces needed in the absence of dorsiflexor in early stance and swing phase. Therefore it is suggested that AFOs prescribed for weakened plantarflexors must be more rigid than ones used for dorsiflexor insufficiency.

Experimental studies of the AFO's stress distribution were carried out by Chu et al. (1996, 1998, 2000, 2001) using strain gauges technology. In a preliminary study Chu (1996) introduced a technique to instrument plastics AFOs based on the UV light treatment of polypropylene surface. She reported that the bonding between strain gauges and polypropylene AFO achieved by this technique was reliable based on her testing results, although no results have been published and no comparison with other measurement techniques have been discussed to state the feasibility of strain gages.

The UV light technique was used as part of surface preparation for the installation of strain gauges on five different custom-made AFO for experimental stress analysis by Chu et al. (1998) Selected motions for swing phase and stance phase were implemented three times for each motion, as testing conditions for the experiment. Results from this study revealed that peak stress concentration in the orthoses varied with a change of the orthosis geometry, and in particular its flexibility. Peak stress concentration, though, was primarily located in the neck region of AFOs.

The aim of another study conducted by Chu et al. (2000) was to determine peak stresses, changes associated with different body weight and to predict if the peak stresses may cause AFO failure. Five strain-gauged polypropylene AFOs were fitted in three subjects of different body weight and data were collected while the subjects performed two of the most common daily activities during rehabilitation, namely, standing up/sitting down, and slow walk. Results shown that the stress measured in AFOs changed in magnitudes and location at different body weights, with stress changes mainly occurred at the neck region. Although the stress recorded in the AFO did not exceed the material yield stress, failure of AFOs due to fatigue can occurs because of a low stress with a high cyclic load (Chu et al., 2000).

In the aforementioned studies strain gauges attached to polypropylene have been used as a measurement technique, although their accuracy is not well documented in literature. It seems that there is a lack of proof regarding the feasibility of strain gauges attached to polypropylene in studies conducted so far.

To this regard Melissa Webster (2006) in a short project carried out in the Bioengineering Department at the University of Strathclyde investigated the application of strain gauges onto polypropylene. Strain gauge values of strain have been compared to those obtained from an extensometer attached onto strain gauged polypropylene samples both UV treated and untreated. Results from tensile tests conducted shown different strain values calculated by the strain gages and the extensometer but the reason for these discrepancies has not been explained.

Further investigations to assess the feasibility of strain gauges attached to polypropylene are required. This in turn needs the availability of another accurate measurement methodology to allow comparisons between data, e.g. have an accurate extensometer. Once the performance of strain gauges is assessed it will be possible to use them to determine stresses generated in AFO and orthotic loads during gait cycles. Evaluate the reliability of strain gauges attached to polypropylene samples will be the first aim of this thesis.

CHAPTER 4

METHODOLOGY AND INSTRUMENTATION

4.1 INTRODUCTION

The measurement of loads actually being generated by the orthosis under normal ambulatory conditions is required to improve design criteria for AFOs. To this regard, the aim of this study was to investigate the use of electrical resistance strain gauges for the evaluation of mechanical performance of a polypropylene AFO under loading.

Strain gauges convert a change in dimension into change of ohmic resistance. From the change in electrical resistance of the strain gauge, usually measured by a Wheatstone bridge, the magnitude of mechanical strain may be inferred.

However before proceeding towards the test of a normal subject fitted with a strain gauged polypropylene AFO, strain gauge technology reliabibility was investigated.

First polypropylene (PP) behaviour under tensile load was investigated. Secondly tests on PP samples with strain gauges attached were conducted. Two different bonding techniques were used to attach the strain gauges. This was necessary due to unsatisfactory results encountered using the first method.

Materials and methods used during the development of this project are detailed throughout this chapter.

4.2 MATERIAL TESTING

Initially, as mentioned above, tensile tests were carried out on polypropylene samples.

Sample were obtained from polypropylene (copolymer) sheets with on average a length of 180mm, a width of 25 mm, and a thickness of 4.5 mm.

Polypropylene specimens were tested using an Instron 5800R tensile testing machine and following as far as possible British Standard BS 527-1.

The main objective of the material testing was to investigate the polypropylene behaviour under tensile loads by means of analysis of stress-strain graphs.

After a sample being clamped on the Instron machine, an extensometer was attached to its side allowing strain measurements. The extensometer was fixed using rubber O'rings to ensure that no slippage occurred between the extensometer and the sample. The extensometer before the start of the testing was calibrated to verify its accuracy. Extensometer measurements were compared with the crosshead movements.

Two different test protocols were created using the software Instron Wavemaker.

First a continuous tensile load from 0 to 1500 N was applied to five samples. The peak load applied, for the calculated cross sectional area, 120.944 mm^2, corresponds approximately to a stress of 12 MPa at approximately 4.8 mm/min.

The choice of 1500 N as maximum load was related to the fact that the viscoelastic nature of the material could be shown in the applied stress range, although 12 MPa is less than the quoted yield strength (Crawford,1998). A previous study (Webster, 2006) was conducted in the Bioengineering Unit under similar test conditions providing additional results for subsequent data discussion. Finally, with a perspective of using polypropylene in AFO manufacture, it is important to have a knowledge of PP behaviour in the stress range likely to be experienced by an AFO. Stresses generated by AFO were found to be at maximum 2 MPa either from experimental study or through a finite element analysis (Chu et al, 1995, 1998, 2000), thus the load applied in this study covers this range.

Using Instron Waverunner the protocol described above created with Instron Wavemaker was applied to five polypropylene samples.

The second protocol created, consisted of 50 N ramp steps of 10 seconds followed by 4 seconds hold step in which the load is maintained constant at the value reached by the previous ramp. The maximum load applied was 250 N. After reaching the peak value a sequence of ramp and hold steps brought the sample back to a 0 load condition. The cycle described was run consecutively 10 times in five polypropylene samples.
Both the continuous load test and the ramp test were conducted under load control.
Two more tests were carried out to further investigate the viscoelastic nature of polypropylene. For these tests two samples under strain control were tested at a low and high strain rate.

4.3 STRAIN GAUGE BONDING PROCEDURE AND TEST SET UP

Four samples of the same dimensions used in the previous material testing were strain gauged and tested.
90° rosette foil strain gauges (Figure 4.1) supplied by Showa Measuring Instruments Company (Tokyo, Japan) were used.

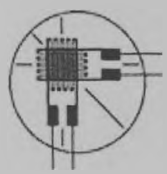

Figure 4.1: Strain gauge used.

Strain gauges were attached on the PP samples using specialised glue, M-Bond AE-10 Adhesive, recommended and supplied by Vishay Measuring Group (USA).
The sample surface where the gauge was to be installed was treated with a No. p240 grit sand paper in conjunction with an acidic cleaner. An alkaline solution was then applied on the surface to neutralize acid particles. References lines for strain gauge installation were marked on the surface spot using a hard pen. The adhesive was prepared following instructions provided by the supplier and applied on the surface allowing strain gauge attachment. A coating agent was finally applied over the strain gauges.

The adhesive features, particularly related to its workability are important when aiming for a correct strain gauge alignment and attachment. Failures will lead to erroneous results.

A full Wheatstone bridge was created on each sample to measure resistance changes in strain gauges and connected to an amplifier (Figure 4.2). Amplifier gain and bridge voltage were set at 200 and 3 V respectively.

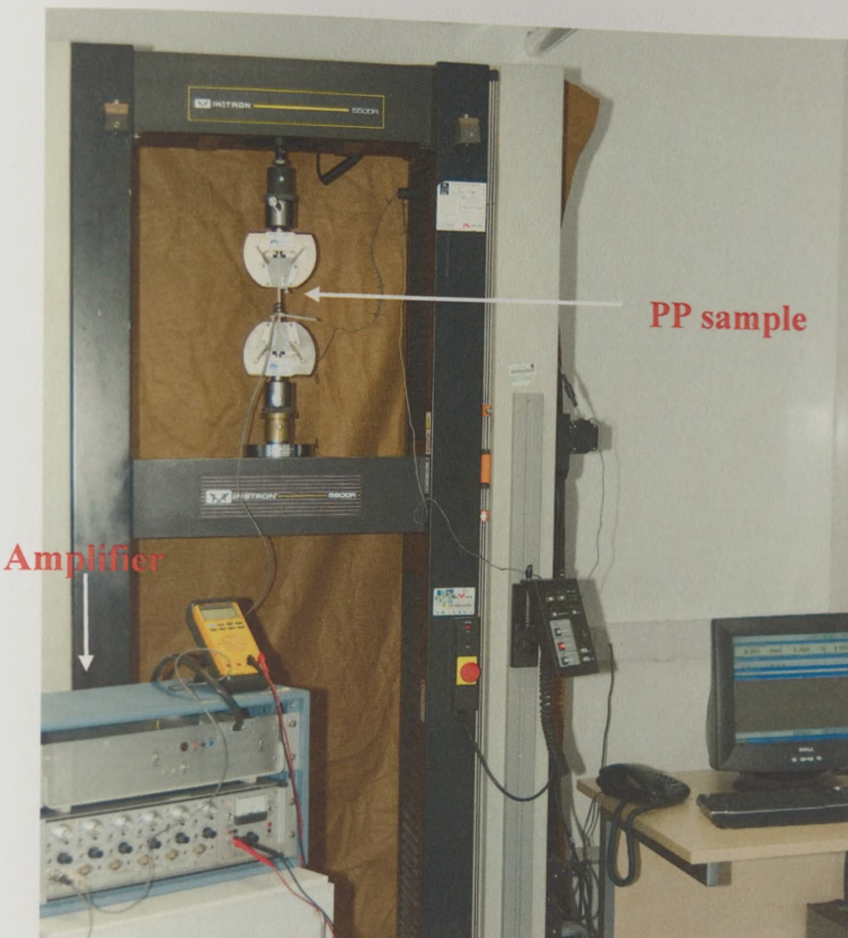

Figure 4.2: Test set up.

In addition to the strain gauges an extensometer was mounted onto a size of the sample (Figure 4.3), after being clamped into the Instron machine. Strains measured by the extensometer were to be compared with strain gauge values to assess strain gauge feasibility of measuring strain in plastic material.

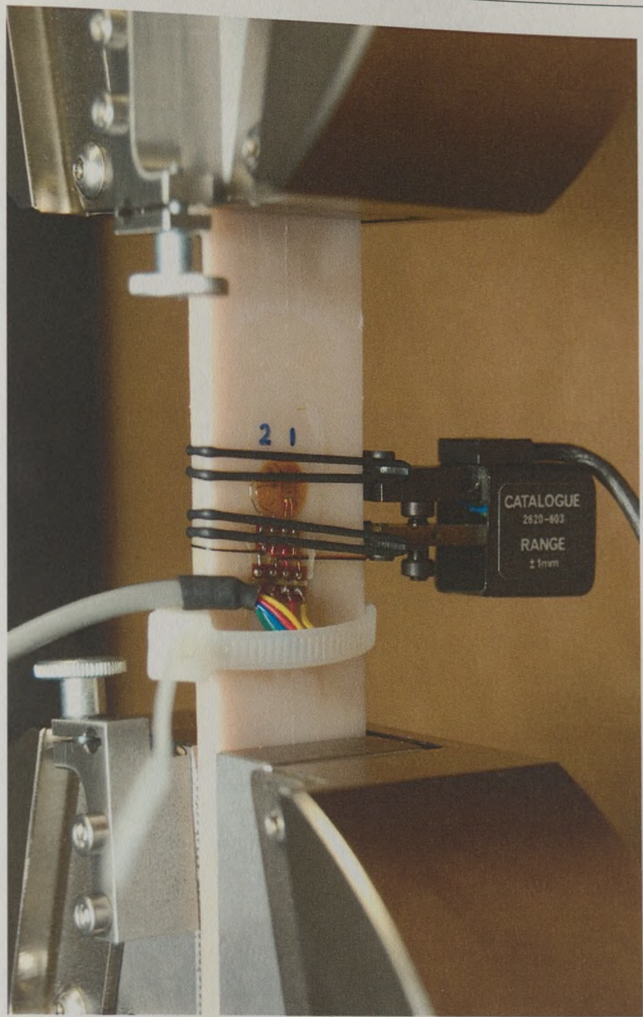

Figure 4.3: Particulars of the sample showing strain gauge and extensometer.

Values of strain from the strain gauges and extensometer, loads applied and crosshead movement were recorded during each test. Data were collected through a Labview program created to allow acquisition of 4 different signals. These signals were transferred to a computer with Labview software install on it by a data acquisition system provided by National Instruments (USA) (Figure 4.4).

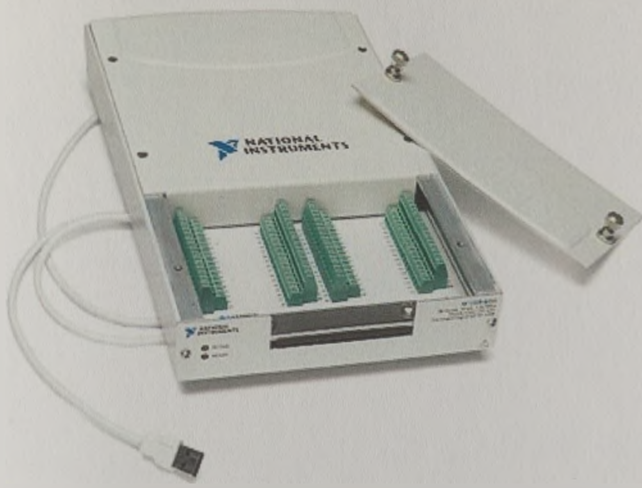

Figure 4.4: Data acquisition system used during tests (USB-6229, National Instruments, USA).

4.4 TEST PROTOCOLS FOR STRAIN GAUGE TESTS

The ramp test protocol created for the material testing was run in each sample at two different strain rates. First a low strain rate test was applied. This test protocol corresponds to a rise time of 10 seconds for each ramp step. Subsequently, the rise time of each ramp was set at 0.5 second, achieving the fastest possible rate to be set in the Instron machine under the given conditions.

Evaluation of the material behaviour under high strain rate is important since an AFO, when fitted in a patient, is likely to experience high strain rate.

Output from the Wheatstone bridge was used to calculate strain values using the following formula derived by the analysis of the Wheatstone bridge circuit.

$$\varepsilon = \frac{2 \cdot e_o}{(1+\nu) \cdot E \cdot K_s \cdot G} \qquad \text{Equation 1}$$

Where: ε = Strain (mm/mm);

e_o = Bridge output (V);

ν = Poisson's Ratio;

E = Bridge voltage (V);

K_S = Gauge Factor;

G = Amplifier Gain.

Regarding the terms on the above equation, the only unknown for the determination of the strain is the Poisson's Ratio. The latter was calculated experimentally as described in the following paragraph.

Details on the derivation of the equation above can be found in Appendix A.

4.5 POISSON'S RATIO

Four tests were conducted to determine the Poisson's Ratio of the polypropylene material. Measurements of both longitudinal and transverse strain were obtained by creating 2 half bridge on each polypropylene sample tested for this purpose. The voltage output of the two bridges was connected to an amplifier. Data were recorded utilizing the system described before for strain gauge testing with the only difference that data from 5 signals were recorded: load, crosshead displacement, longitudinal and transverse strain from strain gauges, and strain from the extensometer.

A tensile test protocol was created. It consisted of a ramp going up to 250 N in 5 seconds, a hold step of 10 seconds and a ramp going back to 0 N. This cycle was repeated 5 times on each sample.

Two polypropylene samples were tested. The load protocol was applied twice on each sample.

The output from the Wheatstone bridges was used to calculate the Poisson's Ratio using its definition:

$$\nu = -\frac{\varepsilon_t}{\varepsilon_l} \qquad \text{Equation 2}$$

Where: ν = Poisson's Ratio;

ε_t = transverse strain;

ε_l = longitudinal strain.

4.6 UV-LIGHT TREATED SAMPLES TESTS

Discrepancies between values of strain calculated from the strain gauge voltage output and values obtained from the extensometer brought about doubts on the accuracy of strain gauge particularly related on the bonding technique used.

Results and pertinent discussion on values comparison are given in the next chapter.

At that stage of the project due to the findings of strain gauge tensile tests, further investigation on strain gauge feasibility were required. The use of UV-light treatment and cyanoacrylic adhesive as bonding technique was, therefore, investigated.

A pre-treatment of the local polypropylene surface with UV-light combined with the use of cyanoacrylate glue has been attempted by Chu (1996). The suggested procedure was then followed during sample preparation.

Spots on four polypropylene specimens where the gauges are to be installed were treated with UV-light. Each sample was exposed to UV-light at a distance of 25 mm for a period of 20-30 minutes. The UV-light source was a CS410-EC UV curing system provided by Thorlabs Inc(Figure 4.5). Strain gauges were then attached using cyanoacrylate adhesive (M-Bond 200), also known as super glue.

Figure 4.5: UV light curing system (Thorlabs Inc.).

The hardware system used during those tests was the same as that developed for the previous strain gauge tests. Thus, it included a full Wheatstone bridge circuit, an amplifier, USB-6229 data acquisition system, and a computer with Labview software.

Each sample, after being clamped on the Instron machine with an extensometer attached on it, was tested with the same protocols as that used in the non UV-light treated samples. A low and high strain rate ramp tests were undertaken.

Before proceeding on the strain gauging of the UV-light treated samples, five samples treated with UV-light where tested to determine whether UV-light exposure altered the polypropylene properties. The continuous load test protocol up to 1500 N, described earlier in this chapter, was applied on five specimens and results compared with those obtained from the untreated samples. A statistical analysis was performed using two sample t-tests for Young's Modulus of treated and untreated samples.

4.7 ALUMINIUM TEST

A further investigation on the use of strain gauges was conducted testing an aluminium sample with a cross sectional area of 34.956 mm^2. The sample was strain gauged using the same gauge foil attached on polypropylene samples, with cyanoacrylate glue (Figure 4.6).

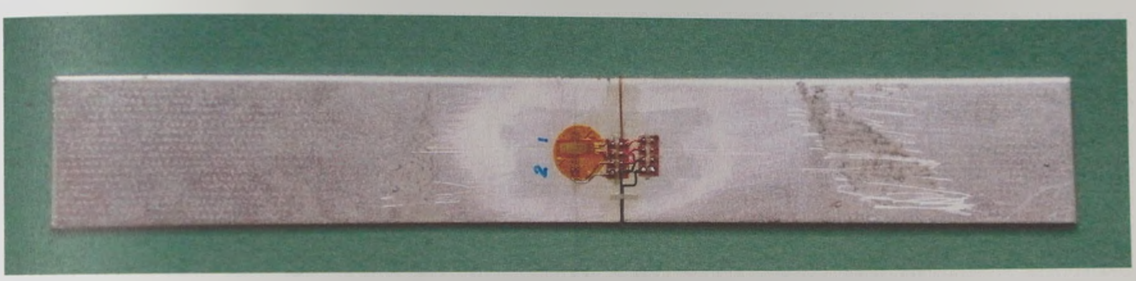

Figure 4.6: Strain gauged aluminium sample.

The test set up and instrumentation for data collection was the same used in previous tests. The aluminium sample was clamped on the Instron machine with an extensometer attach on it and tested.

With the software Instron Wavemaker a new test protocol was created for this purpose. A 10 seconds ramp of 500 N was first applied to the specimen, and hold for 10 seconds and then going back to 0 N in another 10 seconds. Subsequent ramp steps with the same duration of the first one followed by an hold step, were applied incrementing the load each time of 500 N to a maximum of 2000 N. These steps characterizing a cycle were repeated three times in the sample tested. Values of strain calculated from strain gauges voltage outputs and measured from the extensometer were compared.

4.8 STRAIN GAUGED AFO TESTING

A preliminary test with a subject donned with an instrumented AFO (Figure 4.7) was conducted in the gait laboratory in order to calculate forces and moment applied by the orthosis on the subject's leg.

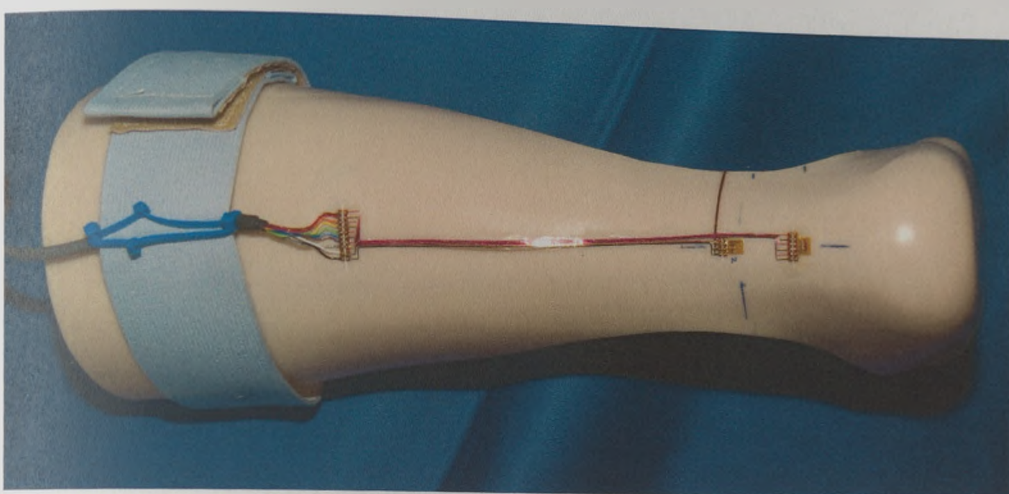

Figure 4.7: Strain gauged polypropylene AFO.

A custom made polypropylene AFO, with about 3 mm wall thickness, was strain gauged using a three-element rosette at 45° connected to create three quarter bridges to allow forces calculation. A full Wheatstone bridge was also made to allow bending moment measurements. The latter, however, differs from the full bridge created on polypropylene samples. The measurement of a bending moment requires, in fact, parallel element strain gauges positioned in both side of the orthosis, inner and outer surface, whereas perpendicular element strain gauges were used in the previous configuration (Figure 4.1) in both sample surfaces. The strain gauges supplied by Showa Measuring Instruments Company (Tokyo, Japan) were attached on the calf region of the orthosis using cyanoacrylate glue. The surface was also pre-treated with UV light, following the method described earlier in this chapter. Figures 4.8 and 4.9, in the following page, show the strain gauged used.

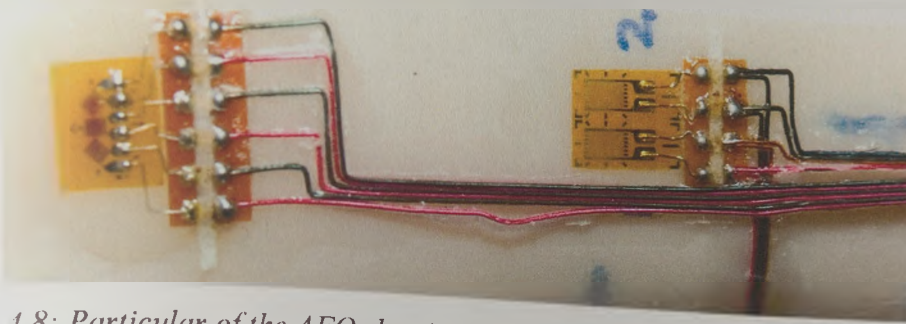

Figure 4.8: Particular of the AFO showing the three-element rosette on the left, and the two parallel element strain gauge used to create a full Wheatstone bridge on the right.

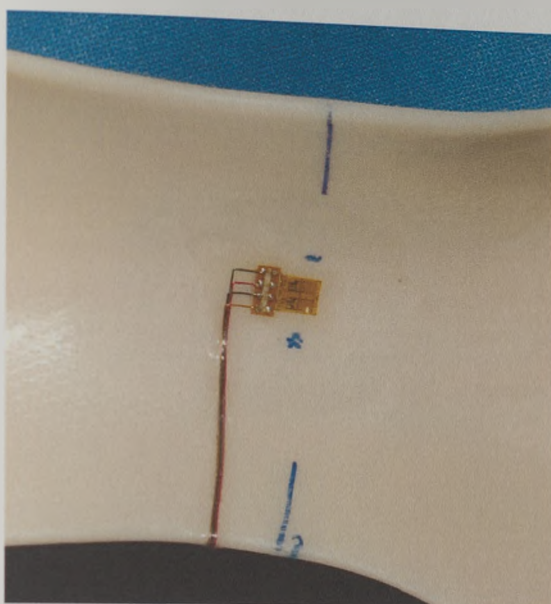

Figure 4.9: Inner surface of the AFO with two parallel element strain gauge connected to the one in the outer surface (Figure 4.8).

Before proceeding towards subject's test, output from strain gauges where checked. At this stage an electrical wiring problem in the rosette circuit reading was encountered. Due to the shortage of time available, it was not possible to adjust the unexpected output and it was, then, decided to move forward the walking trial test measuring only the bending moment and the stress applied in the AFO during walking. The bridge output was connected to an amplifier and then to the Vicon laboratory computer, allowing data recording. Bridge voltage and gain were set respectively to 3 V and 500.

The subject was fitted with the experimental polypropylene AFO and asked to walk throughout the gait laboratory to become accustomed to the orthosis and to precondition the AFO itself. This was necessary because as was shown by previous material tests, polypropylene reaches a steady state after being loaded for a while.

Outputs from strain gauges were recorded while the subject was walking. The data from 5 strides were sampled at a frequency of 120 Hz. An assistant was holding the cables connecting the AFO to the amplifier during the walking trial.

Outputs from one walk were recorded. Although it was planned to record data from more than one walking trial to check the repeatability of the obtained results, the behaviour of the plastic material dissuaded from doing more tests.

AFO calibration was finally performed in order to find the conversion factor to calculate ankle moments from the strain gauge voltage outputs. The AFO was clamped into a grip fixed on a table and a known load applied to it. A hanger of 0.9 kg mass was attached on the AFO in the proximity of the calf section mimic the force that the latter applied on the subject's leg. The voltage output corresponding to that load condition was recorded into the computer and read from a meter connected to the amplifier. Two calibrations were carried out positioning the AFO in a way to reproduce both dorsiflexion and plantarflexion of the ankle joint. The figure in the next page shows the dorsiflexion calibration (Figure 4.10); for the plantarflexion one the AFO was reversed.

Once determined the conversion factor the ankle moment throughout a gait cycle was calculated from the strain gauges voltage output.

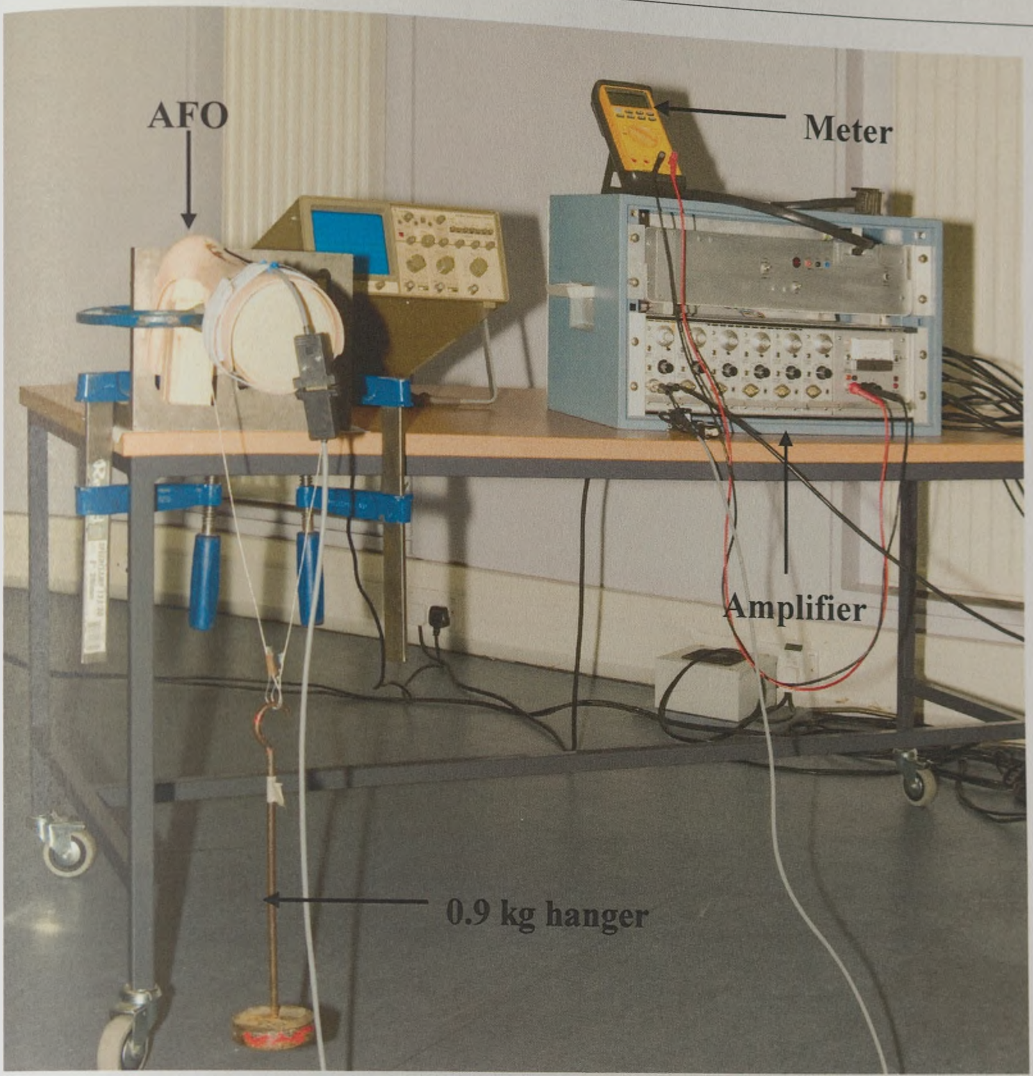

Figure 4.10: AFO dorsiflexion calibration.

The stress corresponding to the max dorsiflexion moment was also calculated. Considering that the load applied is within the linear region of polypropylene, Hooke's law was used to determine the stress generated in the AFO:

$$\sigma = E\varepsilon \qquad \text{Equation 3}$$

Where σ = Stress (N/mm^2);

ε = Strain (mm/mm);

E = Young's Modulus (N/mm^2).

Strain was calculated from the Wheatstone bridge voltage output using the following formula.

$$\varepsilon = \frac{e_o}{E \cdot K_s \cdot G}$$

Equation 4

Where: ε = Strain (mm/mm);

e_o = Bridge output (V);

E = Bridge voltage (V);

K_S = Gauge Factor;

G = Amplifier gain.

Derivation of the equation above is explained in Appendix A.

CHAPTER 5

RESULTS

5.1 INTRODUCTION

The data collected during tensile tests on polypropylene samples both with and without strain gauges attached are given in this chapter together with results recorded during a walking trial of a subject fitted with a strain gauged polypropylene ankle-foot orthosis. Results from the extensometer calibration and aluminium test are also shown.

5.2 EXTENSOMETER CALIBRATION

Extension values measured by the extensometer and crosshead movement of the Instron machine are plotted in figure 5.1. Equation of the best fitted trend line is also shown.

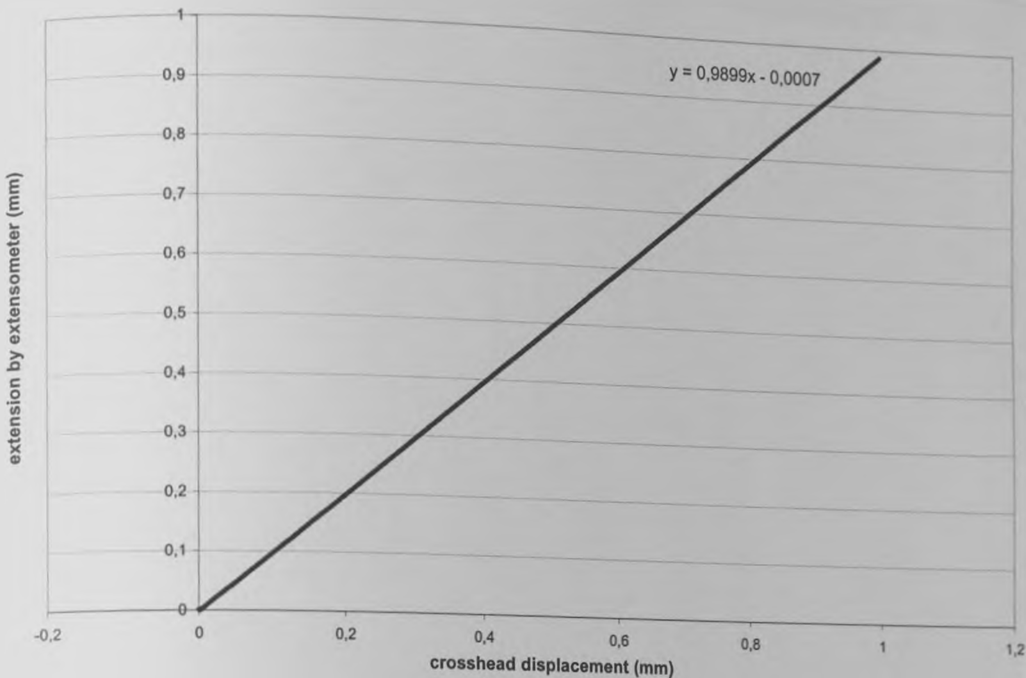

Figure 5.1: extensometer calibration.

The line obtained differs from a 45° line by just about 1.01% demonstrating extensometer accuracy. An approximate strain rate of 2.88 mm/min was calculated.

5.3 MATERIAL TESTING

Data obtained from both the continuous tensile tests, for UV light treated and untreated samples and the ramp tests are given below. In addition results recorded during the further investigation conducted on polypropylene to determine its viscoelastic nature are also shown.

5.3.1 Continuous tensile tests results

Figure 5.2 and 5.3 shows the stress-strain graphs obtained from the tensile testing of untreated samples and UV light treated samples respectively.

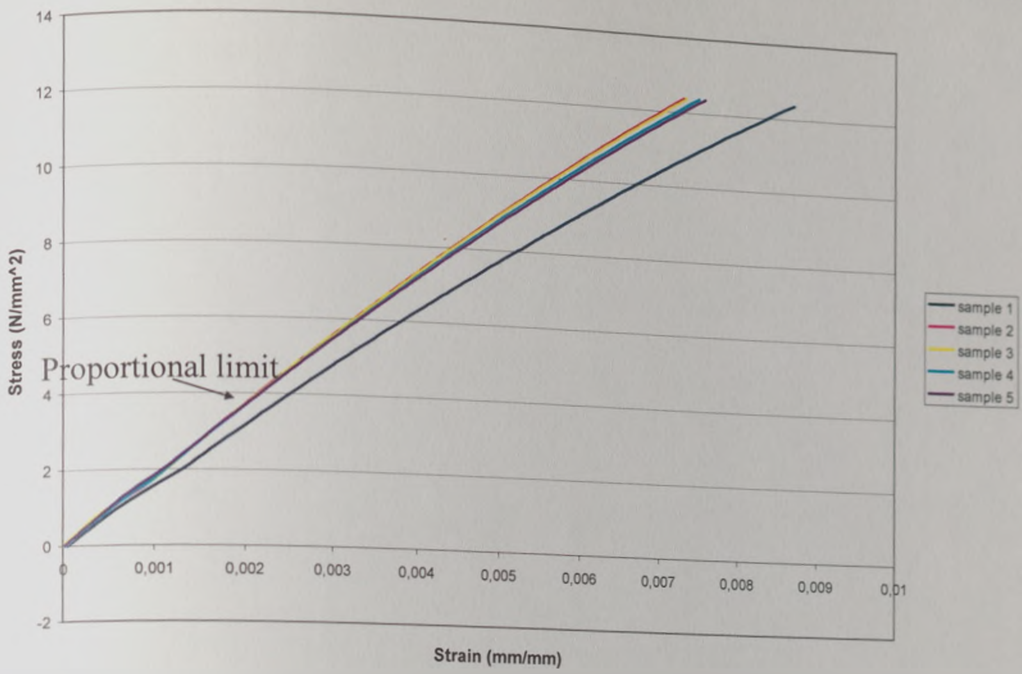

Figure 5.2: Stress-strain graph for the UV light untreated samples for the continuous tensile load test up to 1500 N.

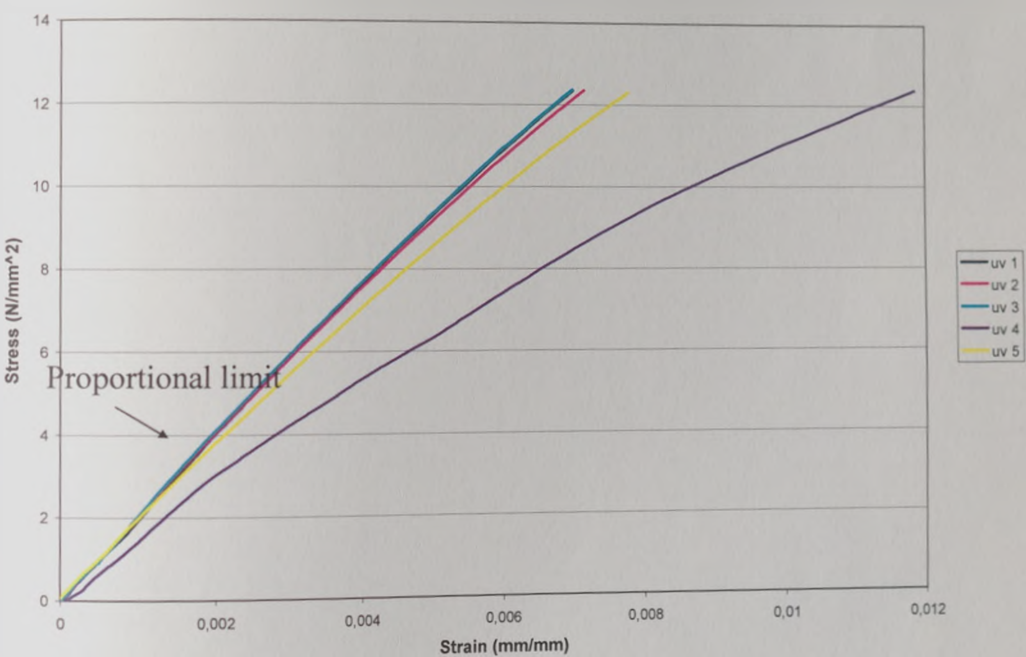

Figure 5.3: Stress-strain graph for the UV light treated samples for the continuous tensile load test up to 1500 N.

In the stress range between approximately 0 – 4 MPa, the stress-strain relationship for polypropylene is linear. This is confirmed by the almost perfect match between the curve and the best fitted trendline in that stress interval (Figure 5.4). As the stress increases, polypropylene begins to show a non-linear stress-strain relationship indicative of its viscoelastic nature. Beyond the proportional limit permanent deformation occurs.

Young's Modulus was calculated by a linear regression procedure applied on the part of the stress-strain curve between two fixed strain values, namely 0.0005 and 0.0025, as described in BS 527-1 (Figure 5.4). Table 5.1 lists the values of Young's Modulus determined for standard and UV light treated samples.

YOUNG'S MODULUS (N/mm^2)					
Standard 1	**Standard 2**	**Standard 3**	**Standard 4**	**Standard 5**	**Average**
1601.2	1905.4	1895.6	1875.7	1829.1	1821.4
UV treated 1	**UV treated 2**	**UV treated 3**	**UV treated 4**	**UV treated 5**	**Average**
2044	2007.4	2059.5	1544.6	1824.7	1896.04

Table 5.1: Young's Modulus found experimentally for UV treated and untreated samples. Standard sample refers to UV light untreated sample.

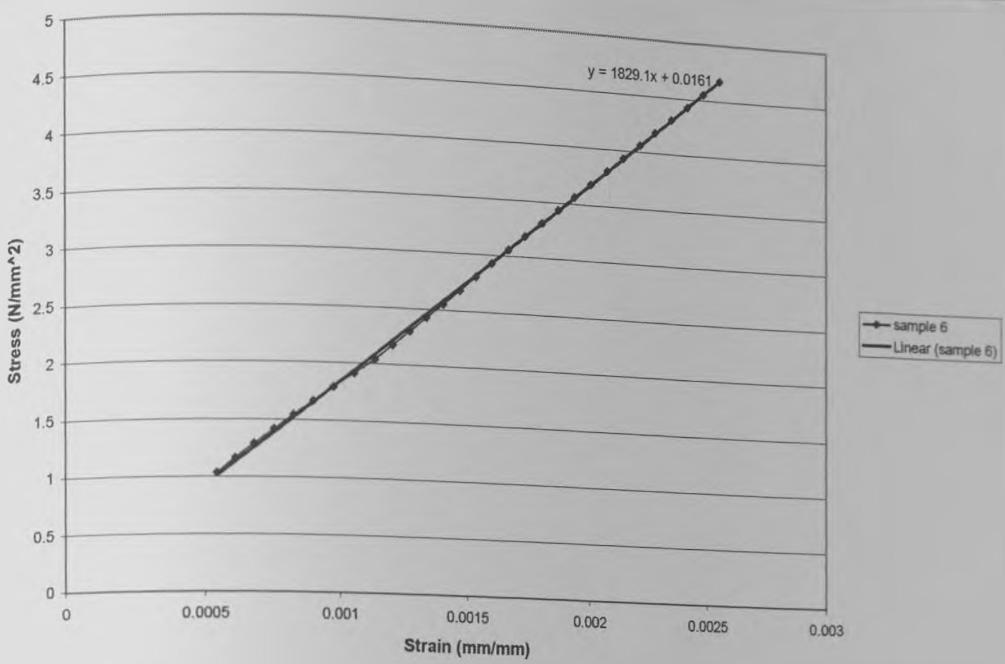

Figure 5.4: Stress-strain graph of the untreated sample 5 in the linear region. The sample was tested with the continuous load protocol.

A two sample t-test at 0.05 level of significance was carried out between the Young's Modulus of standard and UV light treated samples. The p-value obtained (0.53) was greater than the chosen level of significance, showing that there was no evidence to conclude that UV light exposure affects the polypropylene's material properties.

5.3.2 Ramp tests results

Figure 5.5 shows the stress-strain graph of a selected sample for all of the 10 load cycles applied. The results from the other sample were very similar. The graph shows that polypropylene approaches a steady state as the number of cycles increases. This is confirmed by comparing the curves of initial cycles with those of last cycles. Figure 5.6 highlights better the difference between initial and last cycles.

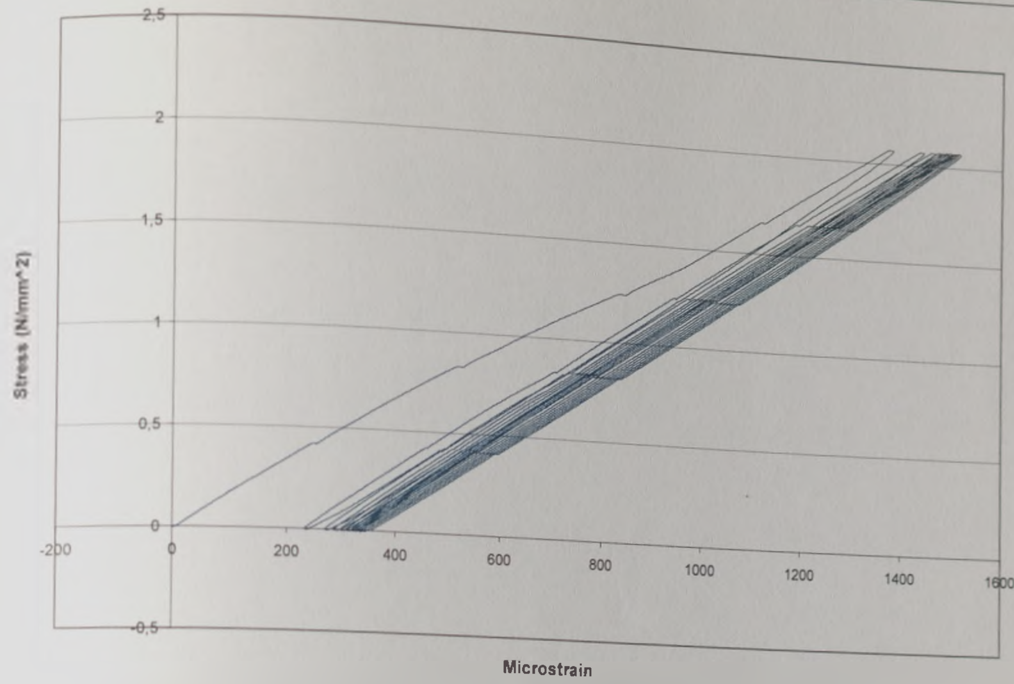

Figure 5.5: 10 cycles stress-strain graph of sample 10.

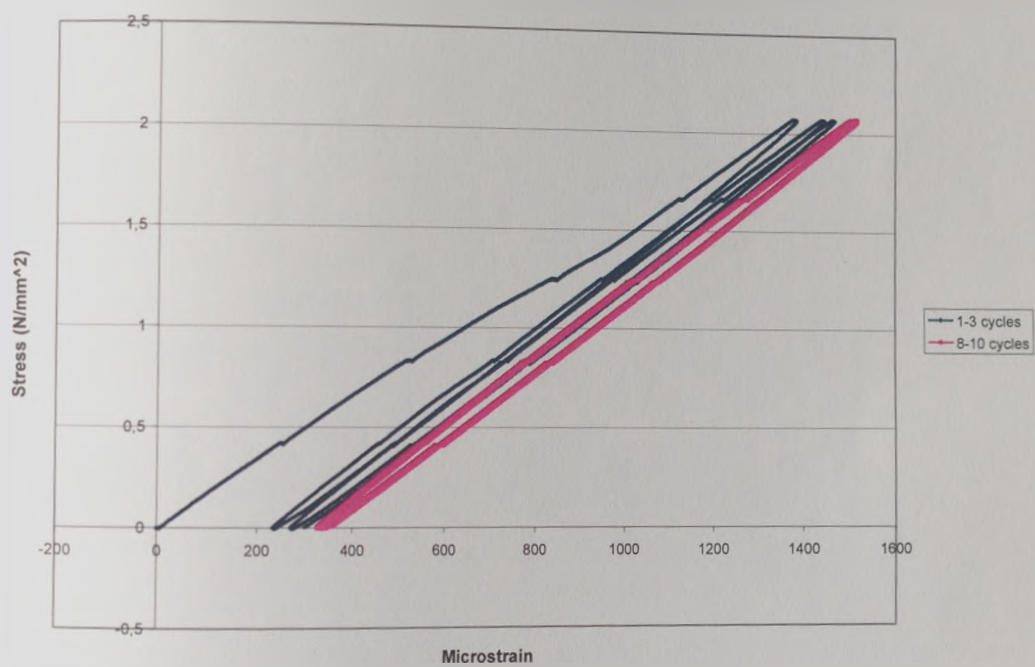

Figure 5.6: Comparison between first 3 cycles and last 3 cycles of sample 10.

In the stress range applied (0 - 2 MPa) polypropylene shows a linear behaviour for both loading and unloading, although they are different. Differences between the two lines and the best fitted trendlines are fairly noticeable (Figure 5.7). Hysteresis occurred and it was more clearly observed as the number of cycles increased in each sample.

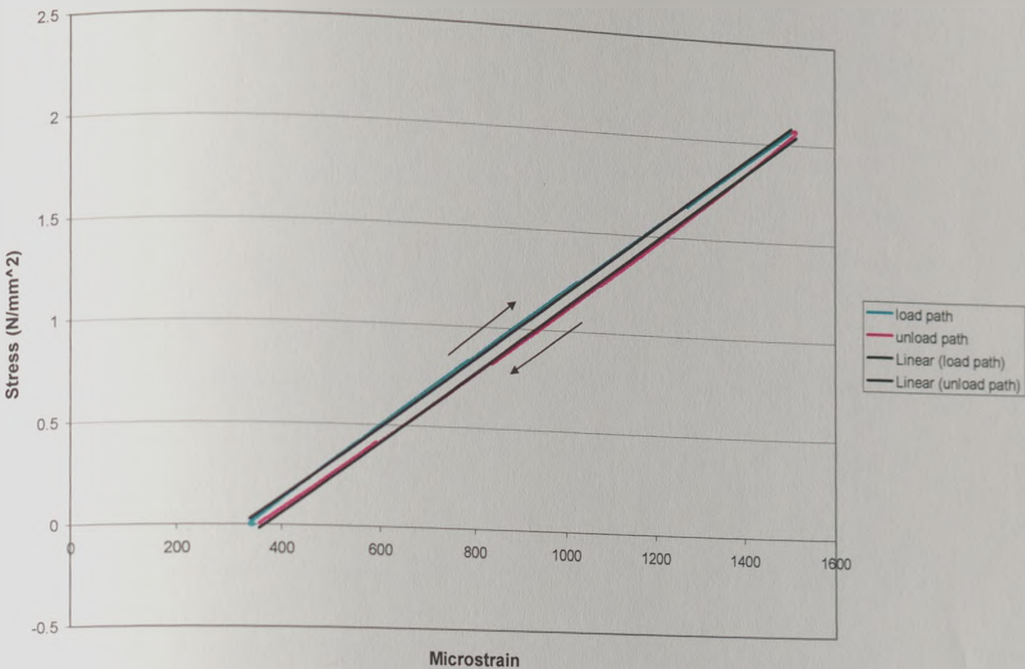

Figure 5.7: Stress-strain graph of the last cycle of sample 10. Arrows indicate the loading and unloading path. Hysteresis is noticeable.

Creep was observed in the results at every hold steps. Figure 5.8 shows the creep during the 4 seconds hold step at 150 N for one of the selected samples. Polypropylene shows a constant response when stress is held stable at each hold steps at successive stress levels. Figure 5.8 represents a detail of figure 5.9, where microstrain is plotted against time showing the constant increasing of strain during 50 N ramp steps once the polypropylene reaches a steady state. Creep is not noticeable in figure 5.8 because the averages of changes in strain during 4 second hold steps are found to be below 0.5% of the maximum strain.

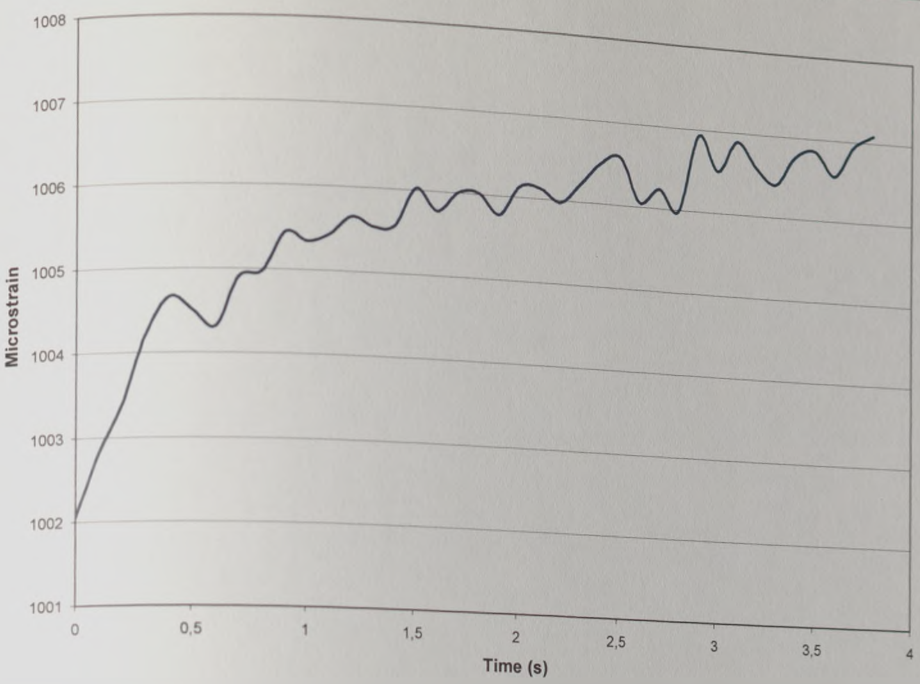

Figure 5.8: Creep during the 4 s hold at 150 N for sample 9.

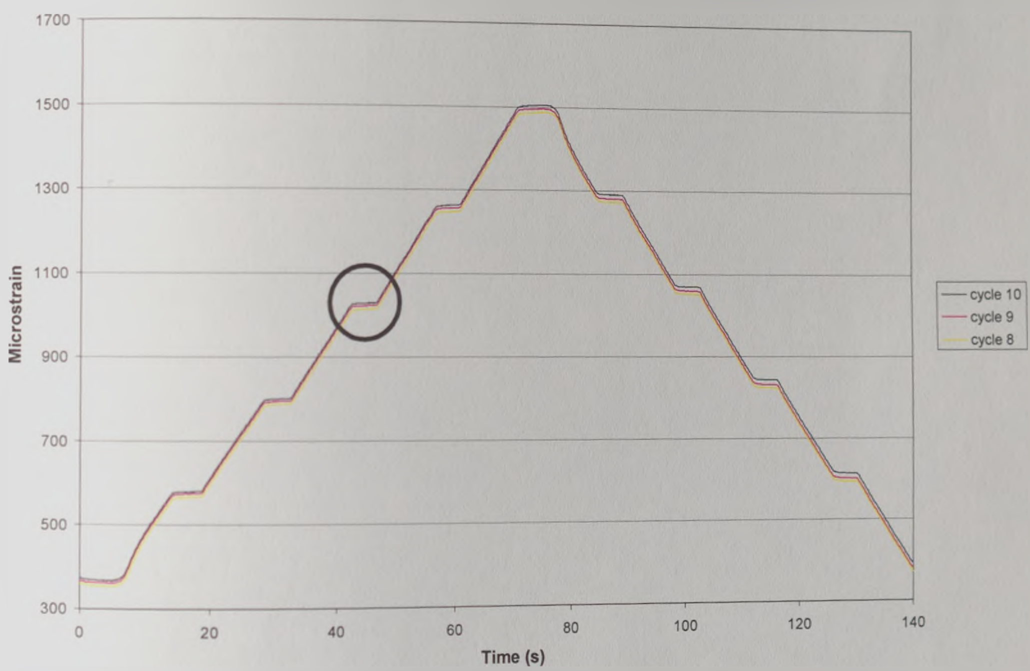

Figure 5.9: Microstrain against time for the last three cycles for sample 9. The circle indicates the creep shown in figure 5.8.

5.3.3 Strain control tests results

Figure 5.10 shows the results of PP samples tested under strain control at a low and high strain rate. The slow strain rate was estimated to be approximately 15 mm/min, whereas the fast strain rate was calculated to be around 956 mm/min. The blue line in the plot illustrates the behaviour of polypropylene when stretched slowly showing the so called cold drawing phenomenon. The test was stopped before fractured of the sample occurred. During the second test the sample broke. The tensile strength for polypropylene under this test condition was found to be 26.7 MPa.

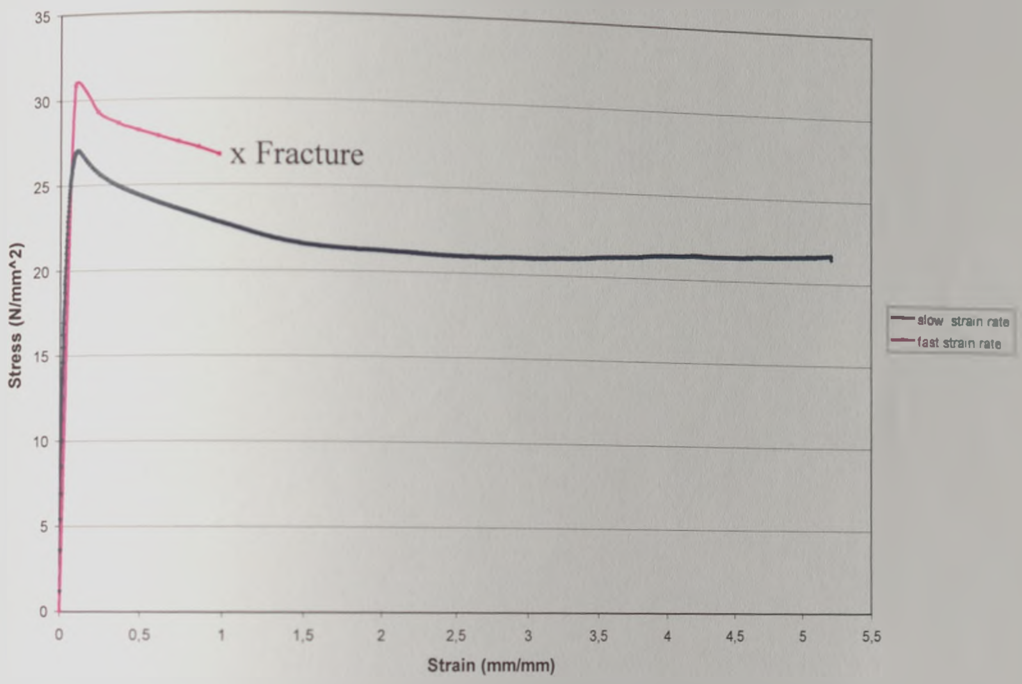

Figure 5.10: Tensile behaviour of polypropylene at low and fast strain rate.

5.4 POISSON'S RATIO CALCULATION

Poisson's Ratio as described in the previous chapter was calculated using its definition in two samples tested twice with the same protocols. The table 5.2 lists the values of Poisson's Ratio calculated. An overall average of 0.42 was found and used for subsequent strain values calculation.

	POISSON'S RATIO	
	Sample 1	Sample 2
Test 1	0.42417	0.42442
Test 2	0.43669	0.40461
Average	0.43043	0.41452
Overall average	0.42247	

Table 5.2: Poisson's ratio found experimentally for the two test samples

5.5 STRAIN GAUGE TESTING

Values of strain calculated from the Wheatstone bridge voltage output using Equation 1 (chapter 4) were compared to strain values recorded from the extensometer for both slow strain rate protocol and the fast strain rate protocol applied on the standard strain gauged samples and UV light treated strain gauged samples. It should be noted that standard strain gauged samples refer to UV light untreated samples with strain gauges attached using M-Bond AE-10 adhesive. Data were, first, filtered using Matlab signal processing software to eliminate noise introduced by the recording system used, before being analysed.

Figure 5.11 compares microstrain values calculated from the strain gauges and measured by the extensometer of a selected untreated sample during the slow strain rate test. The results from the remaining standard samples and UV light treated samples show similar patterns of microstrain throughout the time, also when considering the fast strain rate tests. When plotting microstrain against time a different strain range measured by strain gauges and extensometer is noticeable, with the first one found to be higher than the extensometer measured range. To notice is the approach of a steady state as the number of cycles increases: comparisons of microstrain peak values between consecutive cycles show a reduction in the difference between them until an almost constant value is reached (Figure 5.12). The average of microstrain peak values for the last three cycles for each sample measured by extensometer and strain gauges are listed in table 5.3 and 5.4 for slow and fast strain rate respectively. The standard deviation of maximum microstrain values showed in the mentioned tables, was found to be on average 6.12 and 10.82 for strain gauges and extensometer measurements respectively at slow strain rate, whereas at fast strain rate the averages were 4.51 and 4.53 in UV light untreated samples. Regarding UV light treated samples the following averages of standard deviation were found: 7.25 and 5.54 for strain gauges at slow and fast strain rate correspondingly, while 9.07 and 6.05 are standard deviations for extensometer measurements. Those values are representative of the differences between maximum microstrain values for the last three cycles of each sample and thus they quantify in somehow what was defined "an almost constant value".

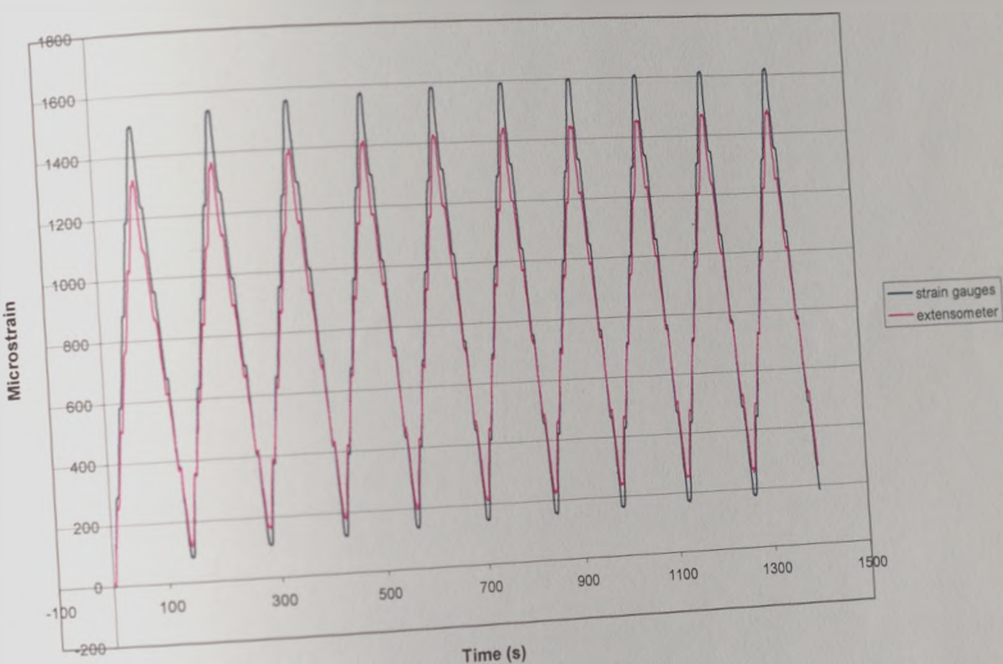

Figure 5.11: Microstrain from strain gauges (blue) and extensometer (pink) against time for the untreated by UV light sample 3 during slow extension rate test.

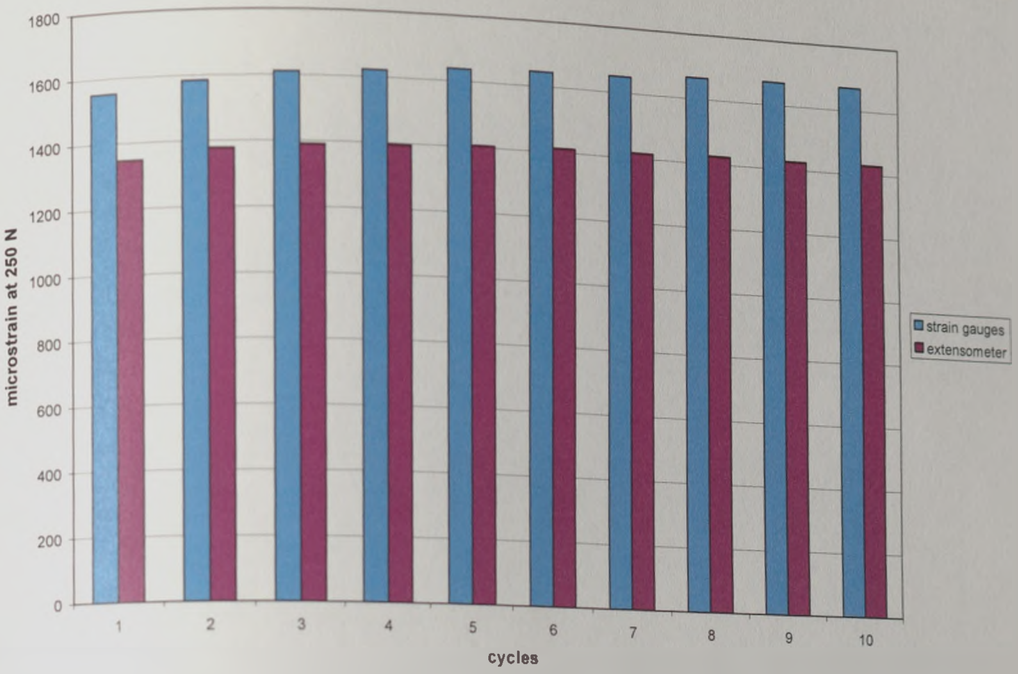

Figure 5.12: comparison between microstrain peak values calculated from strain gauges and measured by the extensometer for untreated sample 4.

Slow strain rate	Sample 1		Sample 2		Sample 3		Sample 4	
	U	T	U	T	U	T	U	T
Extensometer	1423.7	1483.7	1364	1528.7	1460.0	1334.2	1426.9	1421.3
Strain gauges	2529.7	1539.9	1581	1436.9	1608.2	1543.1	1669.7	1472.9

Table 5.3: Average of microstrain values at 250 N for the last three cycles for untreated (U) (M-Bond AE-10 Adhesive) and treated (T) (cyanoacrylate adhesive) samples at slow strain rate.

Fast strain rate	Sample 1		Sample 2		Sample 3		Sample 4	
	U	T	U	T	U	T	U	T
Extensometer	1247.7	1330.5	1214.4	1240.5	1221.3	1281.3	1145.5	1212.3
Strain gauges	1551.7	1462.7	1571.1	1377.4	1545.3	1448.3	1310.9	1392.2

Table 5.4: of microstrain values at 250 N for the last three cycles for untreated (U) (M-Bond AE-10 Adhesive) and treated (T) (cyanoacrylate adhesive) samples at fast strain rate.

The approach of a steady state is better shown in figure 5.13: as the number of cycle increases stress-strain lines are closer to each other, although loading and unloading path are different. Once again the difference between extensometer and strain gauges measurement can be noticed. In the following figures results from the UV light treated sample 2 are plotted. The latter was the only sample in which the extensometer read higher strains than those calculated by strain gauges voltage output. This however occurred only at slow strain rate.

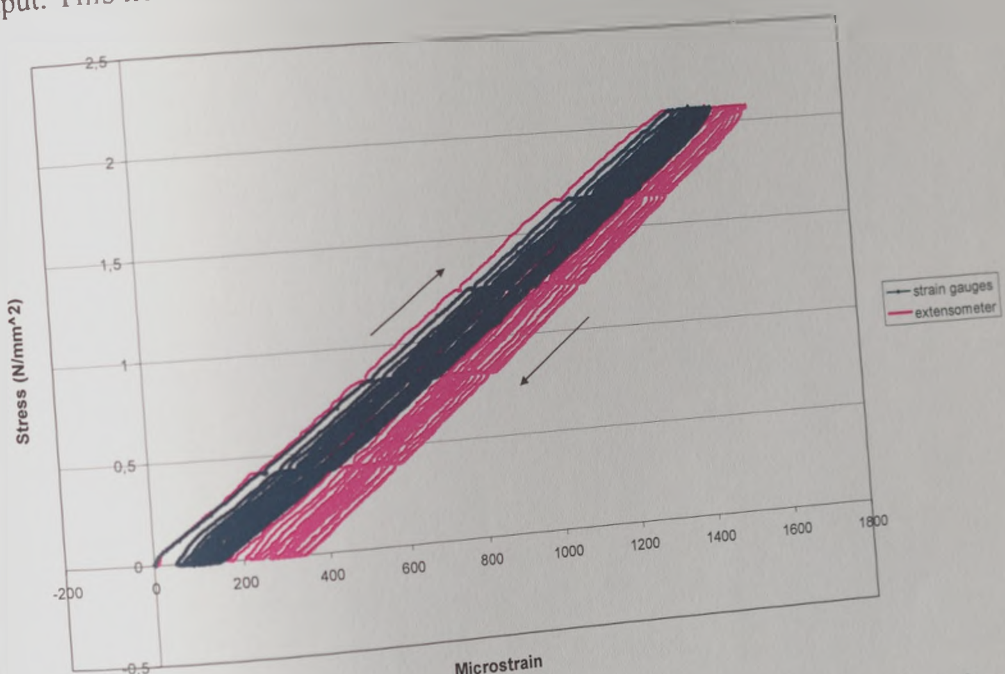

Figure 5.13: Stress-strain graph for the UV light treated sample 2. Arrows indicate the loading and unloading path.

Reliability of the strain gauges was evaluated by calculating the percentage difference between the microstrain range measured by strain gauges and extensometer when polypropylene response to tensile load reaches a constant state. Microstrain range in both the loading and unloading path was, then, calculated for the last three cycles in each sample, and the difference between ranges obtained by the two measurements, strain gauges and extensometer, was evaluated. The averages of the percentage difference of the last three cycles for both untreated and UV light treated samples at slow strain rate are listed in table 5.5. Table 5.6 shows the average differences at fast strain.

Slow strain rate	**Sample 1**		**Sample 2**		**Sample 3**		**Sample 4**	
	U	**T**	**U**	**T**	**U**	**T**	**U**	**T**
Loading	47.10	10.40	16.44	8.05	15.90	15.40	13.03	9.70
Unloading	47.27	8.05	16.25	7.57	16.22	15.58	13.10	9.43

Table 5.5: Average percentage differences between strain gauges and extensometer values of strain for the last three cycles for untreated (U) (M-Bond AE-10 Adhesive) and treated (T) (cyanoacrylate adhesive) samples at slow strain rate.

Fast strain rate	**Sample 1**		**Sample 2**		**Sample 3**		**Sample 4**	
	U	**T**	**U**	**T**	**U**	**T**	**U**	**T**
Loading	21.73	11.02	23.33	15.40	22.64	15.22	13.44	13.03
Unloading	21.8	11.33	33.47	15.65	22.71	15.33	13.56	12.98

Table 5.6: Average percentage differences between strain gauges and extensometer values of strain for the last three cycles for untreated (U) (M-Bond AE-10 Adhesive) and treated (T) (cyanoacrylate adhesive) samples at fast strain rate.

An adhesion problem in the strain gauges of the untreated sample 1 occurred. A gap between strain gauges and sample was noticed when the spring clamp, used just after the strain gauges attachment, was removed. Extensometer measured values of the mentioned sample are comparable with values measured in other samples under the same test conditions. Thus, the problem encountered might lead to erroneous data recorded by strain gauges explaining the high percentage difference between strain gauges and extensometer values.

The results show a better performance of strain gauges attached on UV light treated surface using cyanoacrylate glue. Discrepancies between strain measured by the extensometer and strain gauges are found to be higher at fast strain rate rather than at slow strain rate for both untreated and treated samples.

Figures 5.14 show the results of increasing strain rate for a selected untreated sample in the last cycle. Similar results were observed in the other samples.

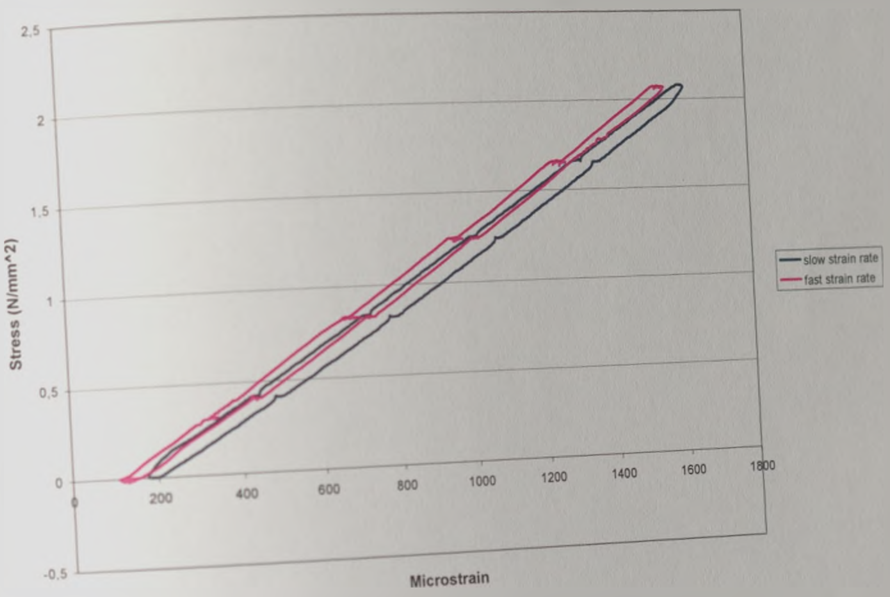

Figure 5.14: Effect of increasing strain rate on the untreated sample 3 in cycle 10

The slow strain and fast strain rates are approximately 0.158 mm/min and 2.43 mm/min respectively. They were calculated considering the increase of displacement at each ramp step for the last cycle, and dividing those values by the interval of time, that was 10 seconds for the slow protocol and 0.5 seconds for the fast protocol.

A comparison between microstrain peak values is shown in figure 5.15. These values were obtained calculating an average of microstrain at 250 N for the last three cycles where repeatability occurs. Values from simple polypropylene samples, treated and untreated samples are displayed in the chart bar below. The aim of this figure was to compare the values in sample with and without strain gauges in the two measurement methods used. The sample without strain gauges is assumed as a standard to which the other samples can be compared. The percentage difference between extensometer values in untreated and treated samples to that of the standard samples was found to be respectively 3.2% and 1.6%. Microstrains from the strain gauges on the other hand, showed a percentage difference of -26% and -2.2% for untreated and treated sample correspondingly. Negative percentages indicate that higher values were recorded by strain gauges than by the extensometer in the polypropylene sample without strain gauges.

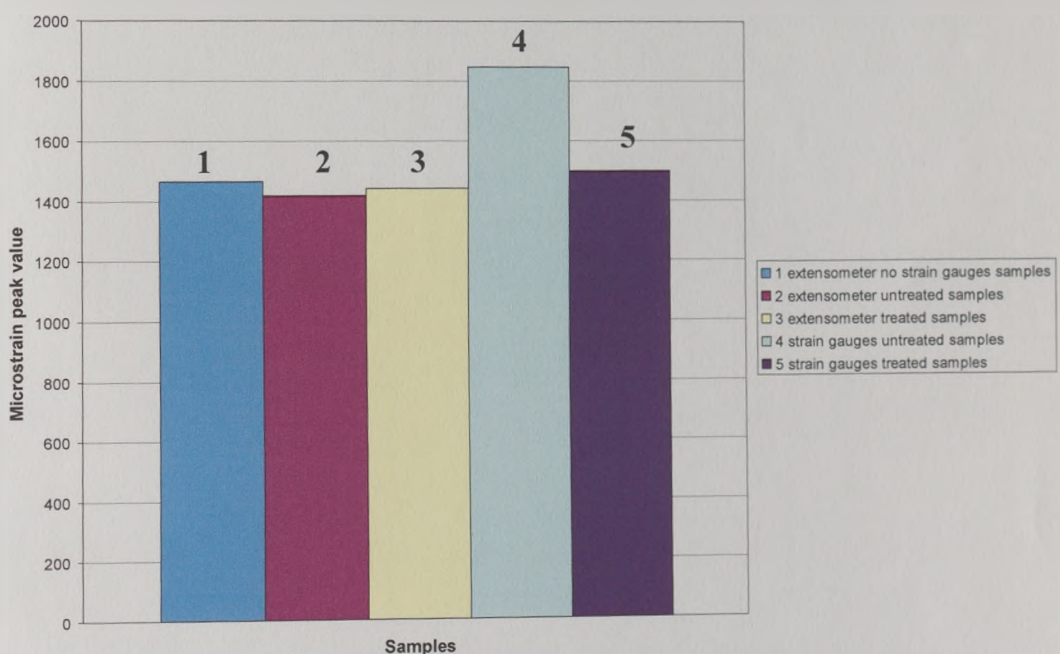

Figure 5.15: Comparison between average microstrain peak values at 250 N measured by the extensometer and strain gauges in the different samples tested.

5.6 ALUMINIUM TEST

Strain values from the Wheatstone bridge voltage output were calculated using equation 1 (chapter 4). A Poisson's ratio of 0.3 was used for the aluminium as quoted in literature. Strain data calculated by strain gauges have been compared to those measured by the extensometer (Figure 5.16). Although the aim of the test wasn't to analyse the aluminium properties, features of that material in contrast to the polypropylene behaviour are easily noticeable from the figure below. First of all any preconditioning phenomenon is observed, repeatability in the values of strain occurs indicating that the sample when unload recovers completely, and no creep was noticed when the load was maintained to a constant value. Although a floating curve is observed correspondingly to hold steps for strain gauges (pink curve in figure 5.16), these drifts can be explained as noise. It is fairly clear in fact that the curve fluctuate around a constant microstrain value. Differently from polypropylene, aluminium show an elastic behaviour for the stress range applied. From an observation of the graph and remembering the one showed for polypropylene sample (Figure 5.11) it seems that strain gauges on metal provide more accurate values than when attached on a plastic material: the two curves in figure 5.16, in fact, follow each other. That statement, however, was verified by the calculation of the percentage difference of microstrain measured by the extensometer and strain gauges (Table 5.7).

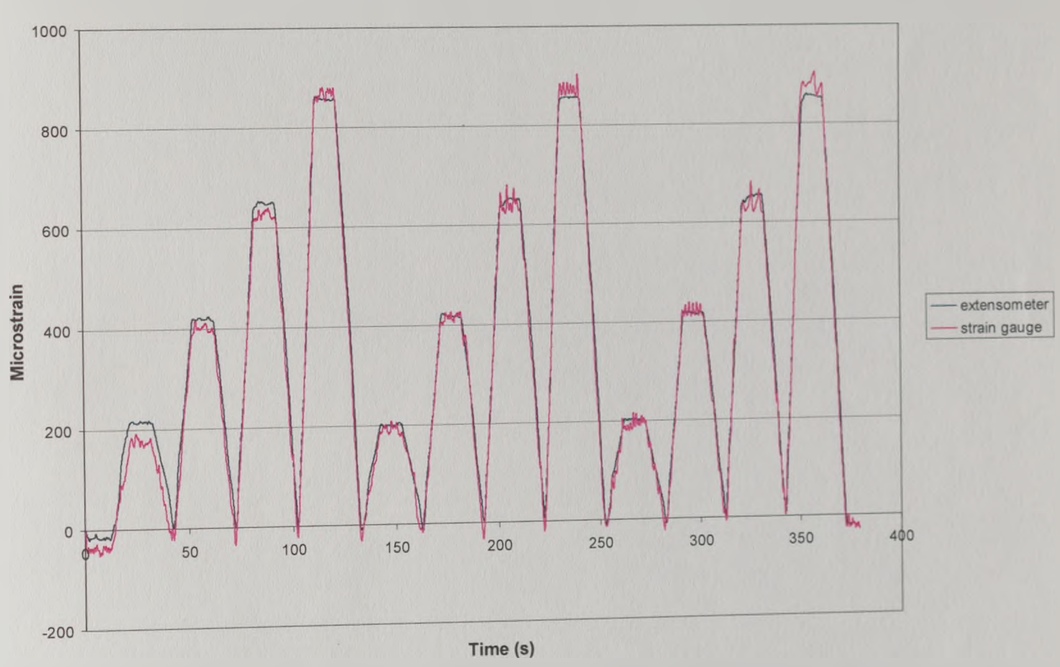

Figure 5.16: Microstrain from strain gauges (pink) and extensometer (blue) against time for the aluminium sample.

	PERCENTAGE DIFFERENCE			
	Load Applied			
	500 N	1000 N	1500 N	2000 N
Cycle 1	-25.12	-4.49	-3.72	0.98
Cycle 2	-3.71	-0.86	-1.10	1.75
Cycle 3	-4.56	0.94	-1.99	2.51

Table 5.7: Percentage differences between strain gauge and extensometer values for the aluminium sample.

An overall average difference of -3.28 was found from the values listed in the table above. A negative value indicates that higher strains were measured by the extensometer.

The next chart (Figure 5.17) shows microstrain peak values of consecutive steps for the 3 cycles applied to the sample. It can be seen that in the majority of the cases (8 out of 12) the extensometer measured higher values, the differences though, as also showed in table 5.7 are minimal.

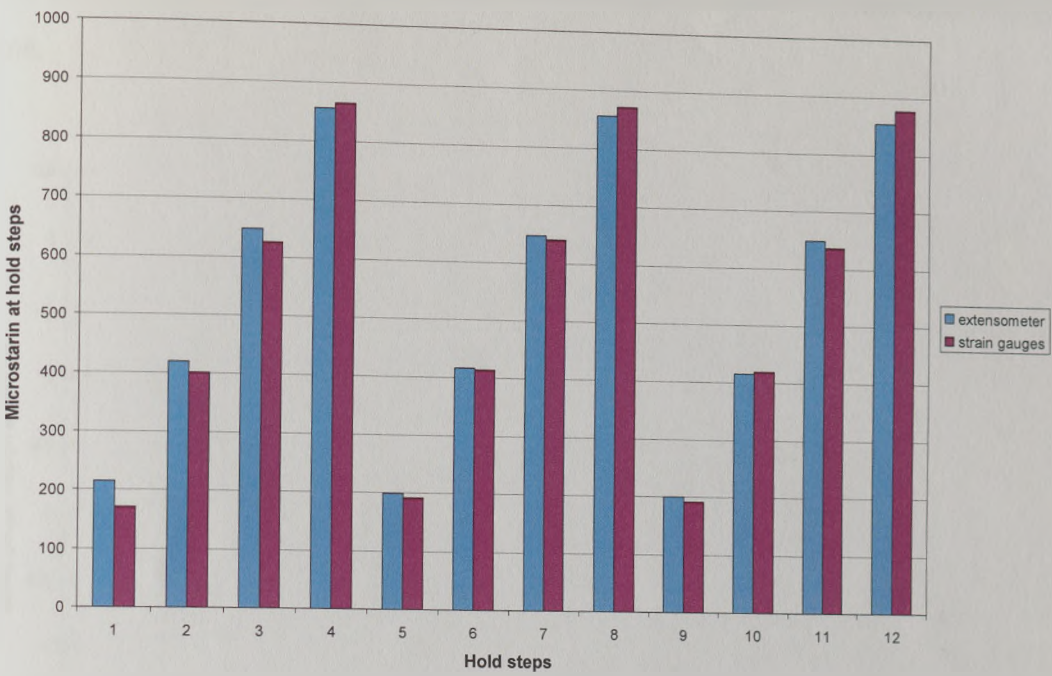

Figure 5.17: Microstrain peak values at 500, 1000, 1500, 2000 N measured by the extensometer and strain gauge during the 3 cycles applied.

5.7 WALKING TRIAL RESULTS

Figure 5.18 shows the voltage output of the full Wheatstone bridge against the experimental time, for the subject fitted with the strain gauged AFO. In particular, the graph displays results relative to four complete strides of the patient's right leg. Before calculate the moments corresponding to the voltages showed in figure 5.18 the calibration factors, both for dorsiflexion and plantarflexion moments, were determined, by means assess the moments that correspond to the voltage output when 0.9 kg were applied to the orthosis. In this way the ratios by which bridge outputs should have been multiplied to work out the moments were found. A leaver arm of 250 mm and 240 mm was measured for the dorsiflexion and plantarflexion calibration position of the AFO respectively. Multiplying those values for the gravitational force due to the weight applied (0.9 *9.81 N), the resultant moments were calculated. A dorsiflexion moment of 2.07 N*m was found, whereas the plantarflexion moment was 2.12 N*m. The related voltage outputs were respectively: 0.43 V and -0.54 V and therefore the ratios were approximately 5.16 N*m/V and

3.90 N*m/V. Figure 5.19 shows moments taken by the orthosis calculated against time.

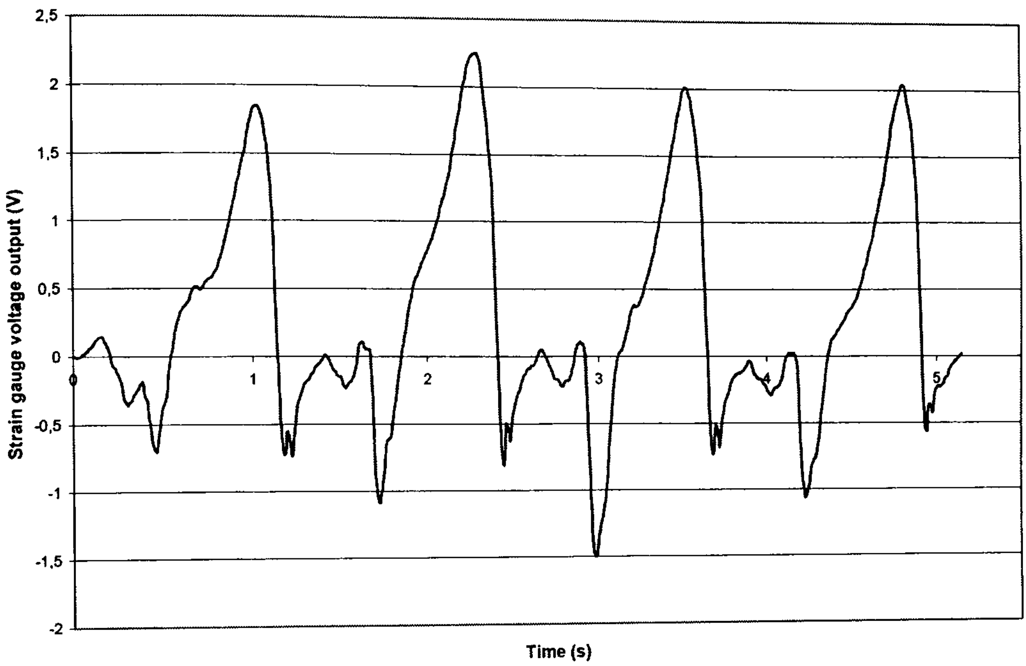

Figure 5.18: Wheatstone bridge voltage outputs during the experimental walking of the subject wearing the instrumented PP AFO.

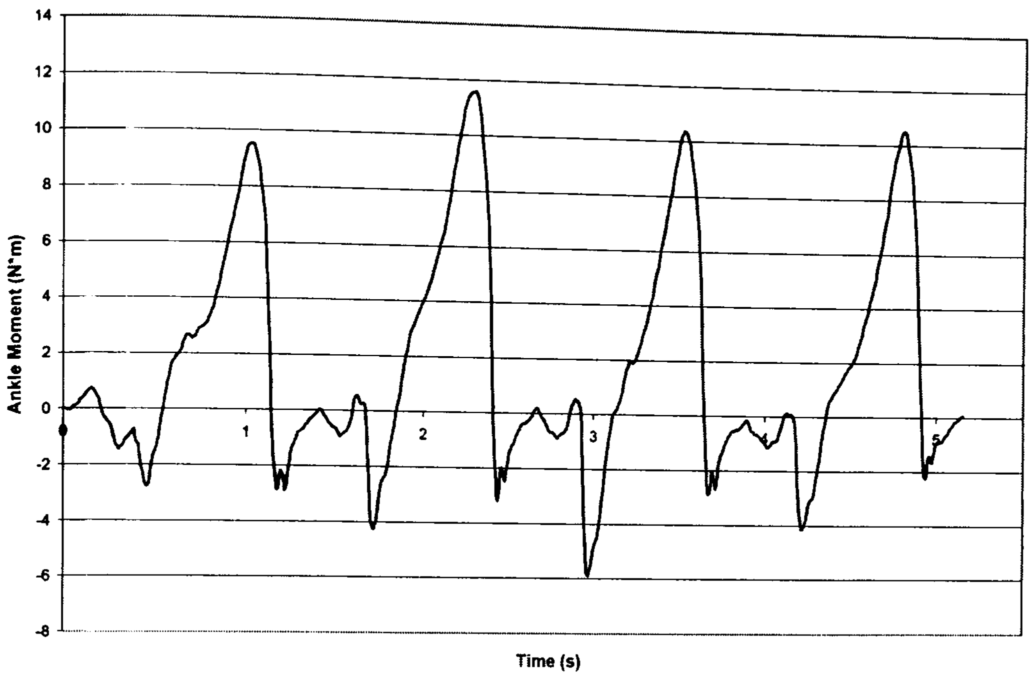

Figure 5.19: Ankle moments taken by the AFO in the sagittal plane. Positive value refers to a dorsiflexion movement of the ankle.

The above graph shows an almost constant pattern for the ankle moment at each stride. Although data from forceplate, mounted below the gait laboratory floor level, were not analysed during this preliminary test, the patient aimed to step up onto it. This explains the highest peak of dorsiflexion moments at the second stride: the subject was concentrating on his following right leg heel strike coincident to the step on the platform. This is also confirmed by the plantarflexion moment obtained which is the highest throughout the conducted walking test, the subject made himself sure to step on the force platform. On average a maximum moment of 10.50 N*m was found.

Ankle moments for a complete gait cycle by the right leg are showed in Figure 5.20.

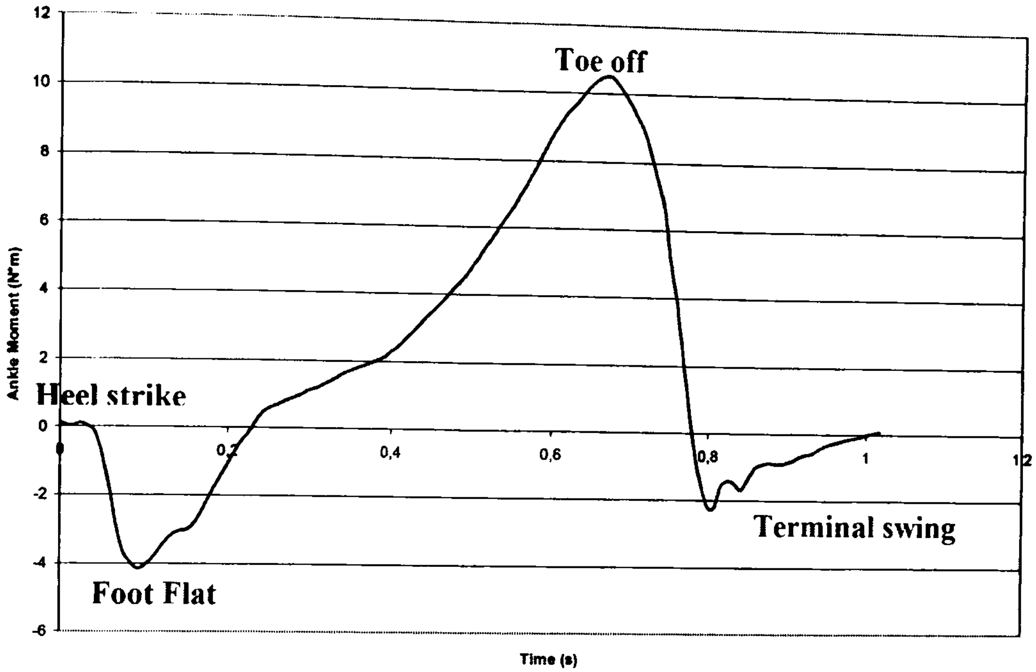

Figure 5.20: Ankle moment during one stride of the right leg.

Regarding the ankle moment for a complete gait cycle (Figure 5.20), the results obtained are in agreement to those observed for a normal gait pattern although different values are showed. This is because what it is showed here is the ankle moment taken by the orthosis, and not the total moment experienced by the ankle, that is referred to be the anatomical ankle moment.

At heel strike ankle plantarflexs. As soon as the foot touches the ground (foot flat) the ankle starts to dorsiflex until the foot leaves the ground at toe off. At this point ankle motion changes rapidly from dorsiflexion to plantarflexion. During terminal swing dorsiflexion occurs again until a neutral position is reached at the end of the gait cycle.

The strain produced by the maximum moment (10.50 N*m) was calculated using equation 4 (chapter 4). A microstrain of 678.77 was found. The stress relative to that strain value was determined with Hooke's law (equation 3, chapter 4), using as Young's Modulus an average of the modulus calculated experimentally (1858.72 MPa). 1.26 MPa was the stress achieved in the AFO at maximum load condition.

CHAPTER 6:

DISCUSSION

6.1 INTRODUCTION

This chapter reviews and discusses the results illustrated in the previous section. First, polypropylene (PP) behaviour under tensile load is discussed. Secondly, comparisons between strain values from the strain gauges and extensometer are analysed in order to comment on the feasibility of use strain gauges for strain measurements on the PP AFO. Finally, results obtained in the experimental trials conducted in the gait laboratory are discussed.

6.2 POLYPROPYLENE VISCOELASTICITY

The initial continuous load tests (Figures 5.2, 5.3) show a linear stress-strain relationship for polypropylene at low stress (0- 4 MPa), whereas at high stress, beyond the proportional limit, there is a non-linear relationship between stress and strain, showing the possible onset of a permanent element to the strain. This is indicative of polypropylene's viscoelastic nature. The properties of a viscoelastic material are time, temperature and strain rate dependent, thus the results gained from these tests would not predict accurately the long term behaviour of polypropylene. In addition, it is important to note that the test conditions will not be the same experienced by an AFO, that will be subjected not only to an uniaxial load at a constant strain rate as applied to the tested polypropylene samples.

Within the linear region the Young's modulus was calculated for treated and untreated samples (Table 5.1). Values found experimentally, on average 1821.4 and 1896.04 MPa for standard and treated samples respectively, fall within the range (1.5

- 2 GPa) quoted for polypropylene. From a statistical analysis, at 0.05 level of significance, it was possible to conclude that UV-light treatment does not alter the material behaviour allowing its use to pre-treat polypropylene surface before strain gauges attachment.

While the first protocol applied to polypropylene samples provide an overview of polypropylene behaviour under a large stress range (0 – 12 MPa approximately), the ramp tests focused on the linear region of the stress-strain graph. These tests, both in samples with and without strain gauges, and both UV treated or not, highlight, once again, the viscoelastic nature of polypropylene. First noticeable indication of this behaviour is the presence of hysteresis (Figures 5.7, 5.13): the stress-strain paths for loading and unloading cycles are different. Hysteresis is related to a loss of energy due to intermolecular bond breakages between the polymer chains that form polypropylene caused by a viscous slippage between molecules under tensile load. As the number of cycles increases hysteresis becomes more evident (Figures 5.5, 5.6, 5.13) with cycles getting closer to each other. Polypropylene thus reaches a pre-conditioned state in which strain values at a given stress are almost constant (Figure 5.12). The approach of a steady state should be taken into consideration when testing an AFO, investigating its property after a pre-conditioned state has been reached.

Although the unloading path does not follow the correspondent loading path they both exhibit a linear stress-strain relationship for the encompassed strain range, as anticipated above (Figure 5.7). The reason why a full recovery to the original length at 0 load condition is not achieved, even though in the linear region, is related to the test applied. In the time allowed polypropylene cannot fully recover; plastic material, in fact, have the ability to recover slowly when the load applied is removed (Crawford, 1998).

Creep, that is one of the most characteristic features of viscoelastic material, also occurred (Figure 5.8) at every hold steps. It was found that for successive hold steps at different stress levels the increase in strain while a constant stress is applied is almost constant (0.5% of the maximum strain). Equally the strain gained at every 50 N ramp steps is approximately the same at different stress levels. Repeatability in strain values occurred in successive cycles when a steady state is approached (Figure

5.9). These reasons might suggest that in the stress range considered, polypropylene has linear viscoelastic behaviour (Crawford, 1998).

Results from the investigation of material properties under different strain rates showed that strain values at a given stress are lower when the samples were tested at a fast strain rate (Figure 5.14). This again, is another aspect of the viscoelastic behaviour of polypropylene, showing the non instantaneous response of the material to an applied load. At fast strain rate polypropylene, as anticipated in theory (Crawford, 1998), appears stiffer than at a slower strain rate. Evaluating the behaviour of polypropylene under a fast strain rate is particularly relevant when considering the use of this material for AFO manufacture. When a subject wears an AFO, the latter will experience high strain rate related to the subject's walking speed that can reach 1.6 m/sec (Rose and Gamble, 2006).

When stretched at slow strain rate, polymeric chains in the polypropylene structure have time to realign themselves (Crawford, 1998). This phenomenon is the so called cold drawing, typical of plastic material behaviour at slow strain rate, observed when a polypropylene sample was stretched indefinitely at a low extension rate (Figure 5.10). This behaviour should be taken into consideration when manufacturing a custom-made AFO. A polypropylene sheet infact is draped over the patient's positive cast, in doing this, polypropylene is stretched. Varying the stretching rate, and thus the strain rate, strength and stiffness properties may change. The pink curve in figure 5.10, instead, is associated to a fast extension rate test. In this situation the sample broke at a tensile strength of 26.7 MPa, a value comparable with those quoted for polypropylene (Crawford, 1998).

6.3 STRAIN GAUGES ACCURACY

The accuracy of strain gauges was ascertained by comparisons of strain values calculated by strain gauges themselves to that measured by the extensometer. Extensometer calibration proved its precision. An almost 45° line was in fact obtained when plotting crosshead displacement against values measured by the extensometer (Figure 5.1). The device used, was then assumed to provide accurate strain measurements valid for comparisons. The two bonding techniques were weighted against each other to assess in some way which methods produce less errors in strain measurements. Regarding to this it was found that the use of UV light treatment combined with cyanoacrylate glue gives better results (Tables 5.5, 5.6), with a reduction in strain gauges accuracy with increased strain rate. In both cases however, values of strain measured by the strain gauges were higher compared to those measured by the extensometer. This finding was somehow unexpected. Reinforcement effects, either local or global, by the gauges on the plastic surface on which they are installed were rather expected (Perry, 1985). If an increase of stiffness occurs following a strain gauge attachment, lower strains will be measured. From the results obtained by these tests it doesn't appear that strain gauges reinforce the surface. Lower values of strain would have been measured by strain gauges also if a slip between the strain foil and a surface took place. This would have been caused by a failed adhesion between the sample and the strain gauge, but again this is not the situation encountered.

When strain gauging a plastic material, the influence of the adhesive on the sample surface must be accounted. The glue itself is a plastic material which posses a viscoelastic nature as the polypropylene it self. This can compromise the accuracy of the measurements. From the comparisons of microstrain peak values (Figure 5.15) it was observed that the strains measured from the extensometer both in untreated and treated samples were close to the value obtained during the material testing, and thus in samples in which no adhesive was used. On the other hand, strains values by strain gauges showed larger discrepancies, especially in untreated samples. This lets one think that there might be some interactions between the adhesive and the strain gauge backing material itself, and this interaction does not compromise the extensometer strains readings. There are factors to which draw attention to justify those differences. In the time available in this project it was just possible to advance some hypothesis that must be verify in further investigations.

When a load is applied to the polypropylene sample polymer chains begin to flow, the adhesive that is a plastic material as well is being stretched together with the sample, strain gauges that are in direct contact with the adhesive layer measure the amount of strain being transmitted by the glue. If the Young's modulus of the adhesive is lower than the one of the polypropylene the strain measured by strain gauges might increase due to the higher deformation experienced by the glue. This effect might be missed by the extensometer because it is not positioned along with the strain gauges on the sample surface. Anyway it is not possible to state that this is the real reason to explain the higher values measured from strain gauges since the adhesive properties in term of Young's modulus and time dependant deformation are not well known.

Ensuring a thinner bonding layer is nevertheless advisable, this is also proved by the results obtained that showed better accuracy when strain gauges were attached upon cyanoacrylate glue. Although the first adhesive was suggested by a major strain gauges supplier (Vishay Micro-Measurement), issues on the workability of the glue, in fact were met. The consequential thicker layer got from the use of the M-Bond AE-10 adhesive might be an explanation of the worse performance of strain gauges. An ideal adhesive should not require clamping after gauge installation (Window, 1992) but the use of the above mentioned glue necessitates of a mechanical clamping whereas for cyanoacrylate, thumb pressure was sufficient to achieve a thin layer. Although the mechanical clamping, it was not possible to achieve a thin adhesive film over the sample surface, as advisable, because the glue showed a rapid polymerisation. Presence of voids in the adhesive line can also be a cause of errors during the measurements. There are indications (Window, 1992) that voids in the glue can results in 'hot spot', and this, in case of plastic samples can cause local loss in specimen properties leading to inaccurate measurements. If this is the situation encountered it will explain the higher values calculated from strain gauges. In contrast, however, a reduction in sample properties should also affect extensometer measurements but this does not seem to happen. It seems again that there is a dealing just between the polypropylene surface and the strain gauge foil, maybe modifying the backing foil properties over which the gauge grid are mounted and thus altering the transmitted strain. Voids just under the backing foil, can alter the strain gauge metal grid behaviour. This will lead to an expansion of the metal due to the increased local temperature and thus to higher strain outputs to be measured. This hypothesis however does not have a strong basis since the presence of voids in the adhesive layer cannot be ruled out and in addition the configuration created in each strain gauged samples should compensate for thermal effects providing the require heat dissipation.

An ideal glue, moreover, should exhibit minimum creep. Regarding to this the increase of microstrain both measured by the extensometer and calculated from strain gauges output during every hold step was observed in each sample. In the majority of the hold steps in treated and untreated samples strain gauges showed a higher creep than that determined by the extensometer, however a not precise pattern in creep amount was found for the samples tested making difficult evaluation of the creep. What can be said is that the creep in samples with an adhesive layer is higher compared to that experienced by polypropylene sample without any glue, especially when considering untreated samples. Also this consideration, thus, may discourage the use of the M-Bond AE-10 adhesive.

Another hypothesis takes into account the gauge length. The gauge length is a strain gauges parameter representative of the area over which strain is measured. The extensometer has a gauge length of 10 mm, while strain gauges of 2 mm and 5 mm length were installed in untreated and treated samples respectively. A strain gauge measures the average of strain over the area covered by the grid, the smaller the gauge the smaller the region on which measurements are concentrated. If the material used behaves uniformly gauge length does not represent a source of errors because the deformation experienced by the sample is the same in each of its parts. If the material behaviour is odd, increasing the gauge length the values obtained will come from an average over a larger area giving lower values than those provided by a more concentrate measurement over the region of maximal strain. Doubts on the uniform behaviour of polypropylene arose. If polymer chains do not stretched evenly the different gauge length of the extensometer and strain gauges can explain the higher strain values calculated by the strain gauge voltage output. This hypothesis is strictly related also to the consideration that extensometer and strain gauges were not positioned over the same surfaces in the samples, besides specimens faces were distinguished by a different superficial finish. Polypropylene samples, in fact, were characterised by polished anterior and posterior surfaces over which strain gauges were attached and by rough lateral surfaces on which the extensometer was positioned. Polymer chains characterising the samples might be stretched differently and the strain over different length from diverse surfaces might consequently varies. Polypropylene behaviour over different areas on the sample can be explain by an uneven stress distribution that might be related to the shape of the sample itself and to the small distance between the region of measurement and the points of load application (figure 4.3) causing stress concentration. If the stress is concentrated over the central area of the sample, strain gauges can measure higher strain values than those measured by the extensometer measuring strain in the proximity of the sample edge. Uncertainties brought about by these considerations must be verified in further investigations.

With the view of use strain gauges for studies on polypropylene AFO a poor workability of the glue used, can lead to a wrong alignment of strain gauges on the surface providing erroneous data. Workability problems, as mentioned before, were encountered during the attachment of strain gauges using M-Bond AE-10 adhesive.

The aluminium test was conducted for the purpose of determining if the discrepancies observed between the strain gauges and extensometer measurements could have been related to the quality of the strain gauges bonding technique used or the polypropylene behaviour itself. The results obtained (Figure 5.16) showed that strain gauges are accurate enough for strain readings on an aluminium sample. A percentage difference in terms of microstrain of -3.28 represents in fact, a satisfactory result. The repeatability of strain values at same load condition was expected since the stresses were in the linear region of the aluminium (Figure 5.17). The fact that constant values for a given load were measured both by, extensometer and strain gauges, put doubts on strain gauge quality and bonding techniques off. This however, is based on a test of one aluminium sample, a larger sample size would have been preferable but due to the limited availability of strain gauges and the restriction in the time allowed for this study it was not possible to conduct more tests.

Considering the modest results obtained by strain gauges attached with the M-Bond AE-10 adhesive on polypropylene samples, the AFO was instrumented using UV light treatment and cyanoacrylate glue. Although differences in measurements persist also with this bonding technique, strains values from strain gauges were not considered totally erroneous to dissuade AFO experimentation.

6.4 COMMENT ON STRAIN GAUGED AFO DATA

As anticipated earlier, the encountered problem that appeared in the 45° element rosettes unabled orthotics forces calculation. During this preliminary study, the AFO dorsiflexion and plantarflexion moments were thus estimated. The results obtained however do not provide valid data for further study comparisons. They, in fact, were obtained from just one walking trial and apparently are strictly related to the particular orthosis used. It should be stated that the orthosis was typical of an AFO that might be prescribed on patient with flaccid paralysis of the dorsiflexor muscles. The results obtained show that strain gauges do not provide completely erroneous data when attached to a polypropylene AFO. Moments graphs (Figure 5.19, 5.20) display the expected pattern for ankle moments in the sagittal plane, although this statement is based on just one walking trial. Polypropylene behaviour in fact was some how unexpected and discouraging in continuing other experimental analysis with the subject donned with the instrumented orthosis. When trying to record the voltage outputs from strain gauges at zero load condition continuous drift on strain gauges readings was recorded and a long recovery time was observed on unloading the AFO. The cause of that it is thought to be due to the thickness of the orthosis itself. The custom made orthosis, in fact, might have been too thin, and thus too flexible and deformable for the load conditions applied during walking. In other words the AFO could have been over stressed, also if the stress corresponding to the maximum moments (1.26 MPa) was found to be lower than the maximum stress (2 MPa) quoted to be generated in a polypropylene AFO by Chu (1998, 2000), however in these studies no details on orthosis thickness and geometry are mentioned, although Chu described the type of AFOs.

A higher number of walking trials are required to assess reproducibility and allow comparison with analogue studies; this unfortunately was not possible in the time available.

CONCLUSIONS AND FUTURE RESEARCH

Improvements in the design criteria for ankle-foot orthoses (AFOs) require an understanding of the mechanical characteristics of the device and its interaction with the lower limb. Nowadays conventional AFOs have been superseded by plastic orthoses mainly made from polypropylene (PP). Investigation on polypropylene AFOs should be conducted and a method by which measure orthotic loads should be studied. The use of strain gauged technology for these purposes, have been investigated in this project.

Because of problems usually involved in strain gauging a plastic material, it is necessary to verify the achievable accuracy of this technology when applied on polypropylene before moving towards an AFO biomechanical study.

In turn, this first step requires the properties of polypropylene to be understood. Tests on polypropylene samples were conducted with the aim of investigating the material viscoelastic properties. Hysteresis, creep and differences in stress and strain behaviour at various strain rates occurred, highlighting material time dependant behaviour.

The investigation on the use of strain gauges for strain measurements on polypropylene sample showed that a better accuracy is achieved when polypropylene is pre-treated with UV light and strain gauges attached with cyanoacrylate adhesive. Comparisons of strain gauges and extensometer values at slow strain rate (0.158 mm/min) showed an average difference of approximately 10% for UV light treated samples and 19% for untreated samples where strain gauges were installed using M-Bond AE-10 Adhesive. At fast strain rate (2.43 mm/min) the accuracy of strain foil is reduced, percentage differences of about 13 and 22 were found respectively for treated and untreated samples. The repeatability on extensometer measured strains brought about doubts on strain gauges reliability on polypropylene confirming again the accuracy of the extensometer as showed by the calibration. Another indication of that inaccuracy of strain gauges is related to the viscoelastic behaviour of polypropylene was obtained by testing a strain gauged aluminium sample. A percentage difference between strains measured by strain gauges and extensometer of -3.28 was found in the aluminium test.

The unexpected finding of higher strain values calculated from Wheatstone bridge voltage outputs compared to those measured by the extensometer requires that further investigations must be done to assess the consistency of the advanced hypothesis. Tests on polypropylene samples using strain gauges and extensometer with the same gauge length should be conducted to verify if the discrepancies found are related to a different local behaviour of the material, which can not be equally read by strain gauges and extensometer if measurements are taken over different lengths. In the tests conducted differences in strain at local level can be related to an uneven stress distribution due to the shape of the specimens been tested in conjunction with the proximity of load application to the area on which strain gauges and extensometer were attached. It is therefore suggested to use a longer sample with a different shape, e.g. dumb bell shaped specimen, to reduced stress concentration and thus strain over particular sample spot.

Scrupulous attention must be placed on the bonding technique used for strain gauges installation when aiming for accurate measurements. Results obtained discouraged the use of M-Bond AE-10 adhesive due to its poor workability and the thicker layer obtained on the surface samples. The adhesive film placed on the sample surface represents a critical parameter to be evaluated to achieve more precise results due to its intrinsic viscoelastic nature that can compromise strain gauge measurements. The properties of the adhesive should be better understood. Adhesive elongation properties should be as close as possible to those of polypropylene; by mean similar Young's modulus so that when a load is applied same strain is generated in the two plastic materials. In addition presence of voids should be avoided to limit thermal effects both in the sample and in the proximity of gauges grid causing higher strains to be measured.

Due to the better accuracy of strain gauges when attached using cyanoacrylate adhesive and UV light surface pre-treatment, the experimental AFO was strain gauged with the just mentioned bonding technique.

Because of electronic wiring problems encountered in the 45° element rosette it was not possible to determine forces supported by the custom-made polypropylene AFO. Moments taken by the orthosis in the sagittal plane were on the other hand calculated. The pattern obtained follows the plantar and dorsiflexion moments for a normal subject during walking. This was a first preliminary study on the evaluation of orthotic loads, further experimental trials should be conducted in order to propose an accurate methods for the study of biomechanical functions of AFOs. The use of an instrumented AFO can be then combined with the use of force plates and kinematic data acquisition system performing a more complete loads analysis of the system AFO-lower limb during gait cycles. In this way anatomical loads can be also evaluated providing important information for an improvement in AFO design criteria and thus functionality.

REFERENCES

American Academy of Orthopaedic Surgeons- AAOS 1985, Orthopaedic appliances atlas, 2nd edition. The C. V, Mosby company, Missouri.

Bowker P 1987, Biomechanics of orthoses, Physiotherapy 73(6): 270-274

Bowker P, Condie DN, Bader DL, Pratt DJ, 1993, The Biomechanics of Orthoses, Ankle-Foot Orthoses, in 'Biomechanical Basis of Orthotic Management'. Butterworth-Heinemann, Oxford.

BS 527-1 1996, Plastics-Determination of tensile properties-Part 1: General principles,British Standard Institution, London.

Cappozzo A, Catani F, Della Croce U & Leardini A 1995, Position and orientation in space bones during movement: anatomical frame definition and determination. Clinical Biomechanics 10(4): 171-178.

Chu TM, Gent AN, Sukthankar S, Reddy NP, 1996, Bonding Methods for Strain Gages on Polypropylene Material.Experimental Techiques, 20(5):29.

ChuTM, 2001,Biomechanics of Ankle-Foot Orthoses: Past, Present, and Future. Topics in Stroke Rehabilitation,7(4):19-28.

Chu TM, Feng R 1998, Determination of Stress Distribution In Various Ankle-Foot Orthoses: Experimental Stress Analysis.Journal of Prosthetics and Orthotics, 10(1):11-16.

Chu TM 2000, Determination of peak stress on polypropylene ankle-foot orthoses due to weight change using strain gage technology.Experimental Techiques, 24(2):28-30.

Condie DN, Turner 1997 An Atlas of Lower Limb Orthotic Practice. Chapman & Hall. London, UK.

Crawford RJ 1998, Plastics Engineering, 3rd edition, Butterworth-Heinemann, Oxford.

Dieli J, Ayyappa E, Hornbeak S 1997, Effect of dynamic AFOs on three hemiplegic adults.Journal of Rehabilitation Research & Development,9(2):82-87.

Finney L, 1997, Investigation into the load sharing and joint stabilising functions of a Knee-Ankle-Foot Orthosis. MSc Thesis. University of Strathclyde, Glasgow.

International Organization for Standardization.ISO 8549-1 1989: Prosthetics and orthotics-vocabulary, Part 1: General terms for external limb prostheses and external orthoses. Geneva.

Lehmann JF 1979, Biomechanics of ankle foot orthoses prescription and design. Archives of Physical Medicine and Rehabilitation 60:200-207.

Lehmann JF, Esselman PC, Ko MK, Smith JC, DeLateur BJ, Dralle AJ, 1983 Plastic ankle-foot orthoses: evaluation of function. Archives of Physical Medicine and Rehabilitation; 64(9): 402-407.

Leone DJ 1987 A structural model for molded thermoplastic ankle-foot orthoses. Journal of Biomechanical Engineering, 109:305-310.

Lim SYE 1985, A study of the biomechanical performance of Knee-Ankle-Foot orthoses in normal ambulatory activities. PhD Thesis, University of Strathclyde, Glasgow.

Magora A, Robin GC, Adler E,Libai A., Eitan A 1968, Dynamic strain analysis of below-knee orthopaedic braces. American Journal of Physical Medicine, 47(1):31-40.

Martini F. 2006 Fundamentals of Anatomy & Physiology, 7th edition, Pearson/B. Cummings.

McHugh B, Cambell J (1987), Below-Knee Orthoses. Physiotherapy 73(8): 380-385.

McHugh B. 1999, Analysis of body-device interface in the sagittal plane for patients wearing ankle-foot orthoses. Prosthetics and Orthotics International, 23:75-81.

Perry J (1985), Strain-Gage Reinforcement Effects on Low-Modulus materials. Experimental Techniques 9(5): 25-27.

Perry J (1992), Gait Analysis, Normal and pathological Function, Benson, USA.

Robin GC, Magora A 1969, Dynamic stress analysis of below-knee drop foot braces; studies on patients with paralysis of the lower limb. Medical and Biological Engineering and Computing, 7: 221-226.

Robin GC, Magora A, Adler E, Saltiel J, 1968, Dynamic stress analysis of below-knee drop foot braces.Medical and Biological Engineering and Computing, 6(5): 533-546.

Rose J, Gamble JG 2006, Human Walking, 3rd edition, Williams & Wilkins, Philadelphia.

Shamp K, Joanne A, 1983,Ankle Foot Orthoses: Metal vs Plastic. Clinical Prosthetics & Orthotics, 7(1):349-351.

Showers David C, Strunck Martha L, 1985, Sheet Plastics and their applications in Orthotics and Prosthetics.Orthotics and Prosthetics: 38(4): 41-48.

Smidt GL 1990, Gait in rehabilitation, Churchill Livingstone, New York.

Webster M, 2006, An Investigation into the Application of Strain Gauges onto Polypropylene. EngD Summer Mini Project. University of Strathclyde, Glasgow.

Whittle MW 2007, Gait analysis: an introduction, 4th edition, Elsevier, Philadelphia.

Window AL 1992, Strain gauge technology, Elsevier Applied Science, Essex, England.

A1: Calculation of strain from Wheatstone bridge voltage output

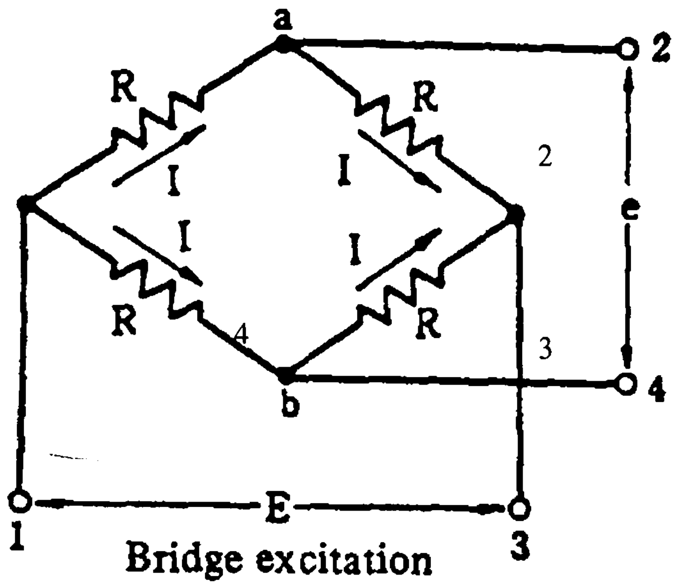

Figure A1.1: Wheatstone bridge circuit.

The Wheatstone bridge is an electrical circuit characterised by four resistance connected to each other. The bridge voltage (E), which was set at 3 V for the tests, is applied between 1 and 3, whereas the voltage between 2 and 4 is the voltage output (e), recorded during the tests. The voltage output, thus is the difference between the potential at the point a and the one at the point b.

$$e = E_a - E_b \qquad \text{(Equation A1.1)}$$

Where E_a is the potential at the point a, defined in according to the Ohm's law as:

$$E_a = R_1 I_1 \qquad \text{(Equation A1.2)}$$

With I_1 being the current flowing through R_1 and R_2. Similarly E_b, the potential in b, is defined:

$$E_b = R_4 I_2 \qquad \text{(Equation A1.3)}$$

With I_2 being the current flowing through R_3 and R_4.

I_1 and I_2 are defined, applying the Ohm's law between the two bridge-arms in which the resistances are connected in series under the E potential:

$$I_1 = \frac{E}{R_1 + R_2} \qquad \text{(Equation A1.4)}$$

$$I_2 = \frac{E}{R_3 + R_4} \qquad \text{(Equation A1.5)}$$

(a) (b)

Figure A1.2: Strain gauges positioning for axial strain reading in both the sample surfaces.

When a Wheatstone bridge is created for reading axial strains (Figure A1.2) the resistances of the bridge are defined as follow:

$$R_1 = R + \delta R \qquad \text{(Equation A1.6)}$$

$$R_2 = R - v\delta R \qquad \text{(Equation A1.7)}$$

$$R_3 = R + \delta R \qquad \text{(Equation A1.8)}$$

$$R_4 = R - v\delta R \qquad \text{(Equation A1.9)}$$

With v being the Poisson's Ratio and ∂R the small change in resistance caused in the circuit b an applied load.

Substituting in equations A1.2 and A1.3 the resistance equations A1.6 and A1.9, and the current definitions (equation A1.4, A1.5), it follows:

$$E_a = \frac{R + \delta R}{R + \delta R + R - v\delta R} \cdot E \qquad \text{(Equation A1.10)}$$

$$E_b = \frac{R - v\delta R}{R + \delta R + R - v\delta R} \cdot E \qquad \text{(Equation A1.11)}$$

Thus e is defined:

$$e = \frac{\delta R + v\delta R}{2R + \delta R - v\delta R} \cdot E \qquad \text{(Equation A1.12)}$$

The latter equation is obtained substituting and simplifying equations A1.10 and A1.11 in equation A1.1. The value $(\partial R - v\partial R)$ is negligible so the formula above becomes:

$$e = \frac{\delta R(1+v)}{2R} \cdot E \qquad \text{(Equation A1.13)}$$

Where $\frac{\partial R}{R}$ is the electrical strain. The latter is related to the mechanical strain in the gauge factor (K) definition as shown:

$$\frac{\delta R}{R} = K\varepsilon \qquad \text{(Equation A1.14)}$$

Substituting equation A1.14 in equation A1.13, and solving the so obtained formula in terms of strain (ε), the required deformation is found:

$$\varepsilon = \frac{2 \cdot e}{(1+v) \cdot E \cdot K_s} \qquad \text{(Equation A1.15)}$$

(a) *(b)*

Figure A1.3: Strain gauges positioning for strain measurements due to bending in both the surfaces of the sample.

When a Wheatstone bridge is created for reading bending strains the resistances of the bridge are defined as follow:

$$R_1 = R + \delta R \qquad \text{(Equation A1.16)}$$

$$R_2 = R - \delta R \qquad \text{(Equation A1.17)}$$

$$R_3 = R + \delta R \qquad \text{(Equation A1.18)}$$

$$R_4 = R - \delta R \qquad \text{(Equation A1.19)}$$

Substituting in equations A1.2 and A1.3 the resistance equations A1.16 and A1.19, and the current definitions (equation A1.4, A1.5), it is obtained:

$$E_a = \frac{R + \delta R}{2R} \cdot E \qquad \text{(Equation A1.20)}$$

$$E_b = \frac{R - v\delta R}{2R} \cdot E \qquad \text{(Equation A1.21)}$$

e is then defined:

$$e = \frac{E\delta R}{R} \qquad \text{(Equation A1.22)}$$

Using electrical strain definition (equation A1.14) in the above formula (equation A1.22) and solving it to calculate the strain, if follow:

$$\varepsilon = \frac{e}{EK} \qquad \text{(Equation A1.23)}$$